The Role of Mouse Barrel Cortex in Tactile Trace Eye Blink Conditioning

Dissertation

zur Erlangung des Grades eines
Doktors der Naturwissenschaften

der Mathematisch-Naturwissenschaftlichen Fakultät
und
der Medizinischen Fakultät
der Eberhard-Karls-Universität Tübingen

vorgelegt
von

Julian Ivo Hofmann
aus Freiburg im Breisgau, Deutschland

Februar 2017

Tag der mündlichen Prüfung: 28.09.2017

Dekan der Math.-Nat. Fakultät:	Prof. Dr. W. Rosenstiel
Dekan der Medizinischen Fakultät:	Prof. Dr. I. B. Autenrieth

1. Berichterstatter:	Prof. Dr. Cornelius Schwarz
2. Berichterstatter:	Dr. Marcel Oberländer

Prüfungskommission:	Prof. Dr. Andreas Nieder
	Dr. Marcel Oberländer
	Prof. Dr. Thomas Euler
	Prof. Dr. Cornelius Schwarz

Erklärung:

Ich erkläre, dass ich die zur Promotion eingereichte Arbeit mit dem Titel:

"The Role of Mouse Barrel Cortex
in Tactile Trace Eye Blink Conditioning"

selbstständig verfasst, nur die angegebenen Quellen und Hilfsmittel benutzt und wörtlich oder inhaltlich übernommene Stellen als solche gekennzeichnet habe. Ich versichere an Eides statt, dass diese Angaben wahr sind und dass ich nichts verschwiegen habe. Mir ist bekannt, dass die falsche Abgabe einer Versicherung an Eides statt mit Freiheitsstrafe bis zu drei Jahren oder mit Geldstrafe bestraft wird.

Tübingen, den ____________________ ____________________________________

Datum Unterschrift

Table of Content

LIST OF FIGURES 1

LIST OF ABBREVIATIONS 2

ABSTRACT 3

INTRODUCTION 5
Associative learning 5
Eye Blink Conditioning 7
Delay eye blink conditioning (DEBC) 7
Trace eye blink conditioning (TEBC) 8
The Whisker System 8
The Whisker Barrel Cortex in Tactile Trace Eye Blink Conditioning (TTEBC) 11
Aim of the study 11

MATERIAL & METHODS 13
Animals 13
Surgical procedure 13
Intrinsic optical imaging 14
Experiments 14
Eye blink performance 16
Electrophysiological implants 17
Electrophysiological recordings 17
LFP/CSD analysis 17
Spike analysis 18
Generalization Paradigm. 19
Fiber implants and optogenetic experiments 19
In some preliminary e 19
Software 20

RESULTS 21
Neuronal activity during TTEBC 22
Motor Signals and Movement Artifacts 26
Spiking and MU activity 27
Generalization to other whiskers 31
Optogenetic Perturbation of BCx during TTEBC 31

DISCUSSION 35
BCx role for TTEBC acquisition and consolidation 35
Neuronal correlate of TTEBC 36
VGAT-ChR2-eYFP mouse line senses transient optogenetic BCx blockade 37
TTEBC generalization across whiskers 38

CORTEX AND CEREBELLUM BOTH STORE THE CS-US ASSOCIATION FOR DIFFERENT PURPOSES. 38

CITATIONS 41

APPENDIX 47

List of Figures

Figure 1. Comparison of delay and trace conditioning 6
Figure 2. The rodent’s whisker system and barrel cortex 9
Figure 3. Behavioral paradigm and setup 13
Figure 4. Physiological methods 15
Figure 5. Eye blink psychophysics 21
Figure 6. Electrophysiology 22
Figure 7. Principal column current source density (CSD) analysis 23
Figure 8. Adjacent and near columns CSD analysis 25
Figure 9. CSD analysis exclusively for not responded (nCR) trials. 26
Figure 10. Multi-unit (MU) baseline activity and CS response 27
Figure 11. MU activity in the principle barrel 28
Figure 12. Firing rate changes during TTEBC 29
Figure 13. Generalization to neighboring whiskers in TTEBC 30
Figure 14. Optogenetic BCx blockade during TTEBC acquisition and retention 32
Figure A1. MU activity on the first shank 47
Figure A2. MU activity at a distance of 200µm (2nd shank) 48
Figure A3. MU activity at a distance of 400µm (3rd shank) 49
Figure A4. MU activity at a distance of 600µm (4nd shank). 50

List of Abbreviations

AUC	area under the [Receiver operator characteristics] curve
BCx	barrel cortex
Cb	cerebellum
ChR2	channelrhodopsin-2
CI	confidence interval
CR	conditioned response
CS	conditioned stimulus
CSD	current source density
Cx	cortex
DEBC	delay eye blink conditioning
EBC	eye blink conditioning
eYFP	enhanced yellow fluorescent protein
FC	fear conditioning
GABA	*Gamma*-aminobutyric acid
i.p.	intraperitoneal
IQR	interquartile range
ITI	inter trial interval
L1 to L6	layer 1 to layer 6
LFP	local field potential
M1	primary motor cortex
MU	multi-unit
nCR	non-conditioned response
S1	primary somatosensory cortex
S2	secondary somatosensory cortex
s.c.	subcutaneous
sd	standard deviation
TEBC	trace eye blink conditioning
TTEBC	tactile trace eye blink conditioning
UR	unconditioned response
US	unconditioned stimulus
VGAT	vesicular GABA transporter
WM	white matter

Abstract

Mouse whisker-related primary somatosensory cortex (also known as barrel cortex, BCx) is required to form an association between a behaviorally relevant tactile stimulus and its consequences, only if the first conditioned stimulus CS (here a single whisker deflection), and the latter unconditioned stimulus US (here a corneal air puff) are separated by a 'trace' (brief memory period). I investigated whether tactile trace eye blink conditioning (TTEBC) has a correlate in BCx activity and whether such BCx activity in the two periods, CS and trace are required for learning.

I trained three head-fixed mice on TTEBC to assess learning related functional plasticity of BCx by recording LFPs and multi-unit (MU) spiking from 4-shank laminar silicone probes (8 electrodes per shank, inter-shank distance 200µm) spanning the depths of the principal barrel column and its neighbors. Current source density analysis (CSD) showed the known short latency sink (~8ms) in L4 and L5/6 during CS presentation, followed by a weaker current sink during ongoing tactile stimulation, spanning across the column. At the same depth, a novel current source was discovered during the trace period. The latter two currents were consistently attenuated during TTEBC acquisition. Onset MU spike response to the CS (at a latency of <15ms) was stable in most units, while steady state CS-response (50-250ms) typically decreased below the pre-learning level. Spiking during the trace period also depressed during learning. These plastic changes were observed in neighboring shanks at a horizontal distance of up to 400µm. These findings show that BCx is functionally involved in TTEBC acquisition. Matching the lateral spread of the neuronal signal into the neighboring column, I found mice to generalize the CS-US association only to adjacent, but not to near and far whiskers.

I next asked whether the involvement of BCx during the trace period has any causal role in TTEBC. I employed the well-established VGAT-ChR2 mouse line that, due to expression of channelrhodopsin-2 in inhibitory neurons (Zhao *et al.*, 2011), blocks virtually all spikes in a column with high temporal precision, using blue light. I found that BCx functionality was required during CS presentation. However, mice learned normally when blocking BCx during the trace period. After learning, BCx activity during CS & trace was entirely dispensable for task performance.

In summary, I demonstrate that the barrel column is involved in acquiring the TTEBC association. Nevertheless, the plasticity of the neuronal response in the trace period is a non-causal reflection of learning, and after learning, in the early phase of retention BCx is not needed for task performance. Future research need to establish if BCx assumes a more critical role in late consolidation. Further, the nature and projection of the signals measured during the learning have to be explored on the microscopic network and cellular level.

Introduction

Associative learning

The temporal or spatial connection of conceptual entities and/or mental states is called association. In other words – associative learning links ideas together, which subsequently reinforce each other. Through associative learning, a behavior can be acquired or modified, based on its importance for an individual. In an environment that changes during the lifetime of an individual, associations can be essential for survival, as they allow the event-based prediction of positive and negative consequences i.e. the presence of: an appetitive stimulus (e.g. food), or an aversive stimulus (e.g. predator). Associations can be already formed, and later recalled, by a single pairing of events – i.e. 'episodic learning' or 'episodic memory'. Note, that episodic memories are often key events that are well remembered. Otherwise, associations require 'conditioning', i.e. the repetitive occurrence of a stimulus and a response. Depending on whether the acquisition of information can be spoken out – or not, we distinguish between 'procedural' and 'declarative learning', respectively.

In mammals episodic and declarative ('explicit') learning typically require the hippocampus and neocortex, while procedural learning can be done with subcortical structures alone. The present study focusses on mammals and cortex function, but it needs to be emphasized that associations and even higher learning capabilities are not bound to the expression of a cortex or cortex-like structure in the animal kingdom (e.g. Giurfa, 2015). Even plants, some argue, may have a basic capability of association (Gagliano *et al.*, 2014).

A typical example for procedural learning or memory is motor skills/motor learning that is subconscious. As said, this type of association learning happens independent of cortical contributions (albeit subjects may nonetheless be able to report about the contingencies of the pairing/stimuli (Clark & Squire, 1998)). In contrast, declarative learning and memory is a conscious process that recalls prior information. Acquisition and storage of explicit memory can be split into three phases: acquisition, 1st consolidation, and 2nd consolidation (Grosso *et al.*, 2015). As the initial step, during acquisition, hippocampus in concert with cortex (Cx; hippocampal-cortical circuits) and other brain regions are thought to be the major carrier for a new association. Any recall in the immediate past of association (i.e. 'recent memory'), requires hippocampus function. As the association matures, in the 1st consolidation phase, hippocampus becomes less and less important, with a broad cortical network holding the memory. Weeks later, as a result of the 2nd phase of consolidation, association retrieval (i.e. 'remote memory') is refined to only a subset of the former used Cx areas (Frankland & Bontempi, 2005; Grosso *et al.*, 2015). (Note, that hippocampus may also govern some forms of procedural learning; Schendan *et al.*, 2003; Christian & Thompson, 2003; Henke, 2010)

Animal experiments traditionally test associative learning using fear conditioning (FC) and eye blink conditioning (EBC) as classical Pavlovian conditioning paradigms. Here associations (measured by e.g. freezing behavior and eye blinks, respectively) are highly motivated by negative emotions due to the aversive nature of the tasks (‘aversive learning’). In fact, inactivation of the amygdala, a major structure dealing with signals of emotion, hinders the acquisition of aversive associations (Helmstetter & Bellgowan, 1994; Siegel *et al.*, 2015). Offering the complementary approach, appetitive training uses positive reinforcement (in form of e.g. water/food). Here, emotional motivations are weaker than in aversive paradigms, with opponent interactions between aversive and appetitive motivations (Barberini *et al.*, 2012; Nasser & McNally, 2013).

Amongst the associative learning paradigms, EBC is one of the best understood, in terms of underlying brain structures and circuits. Compared to FC, it is less affected by (confounding) emotions and experimentally nicely accessible by tightly controlling CS properties and easy US read-outs as eyelid movement. In this study I combined it with head-fixed electrophysiology and optogenetics attaining highest possible experimental control.

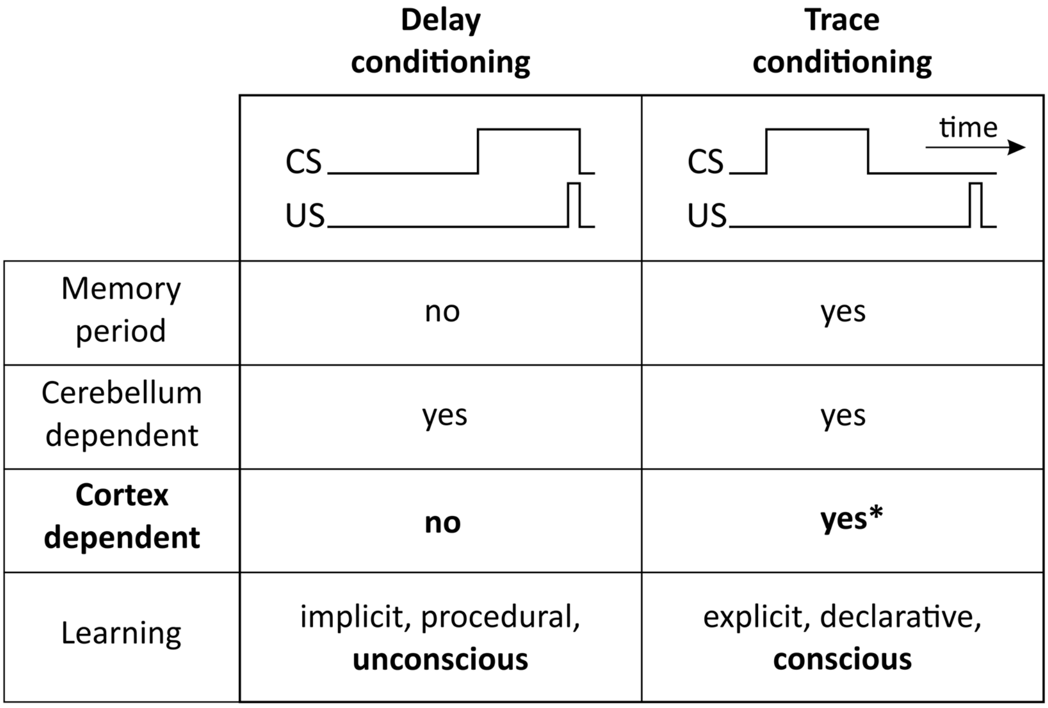
CS
US
CS
US
time

	Delay conditioning	**Trace conditioning**
Memory period	no	yes
Cerebellum dependent	yes	yes
Cortex dependent	**no**	**yes***
Learning	implicit, procedural, **unconscious**	explicit, declarative, **conscious**

Figure 1. Comparison of delay and trace conditioning. *Delay conditioning is characterized by a co-termination of the conditioned (CS) and the unconditioned stimulus (US), while trace conditioning exhibits a temporal gap between CS and US, creating a period during which a short-term memory (the ‘trace’) must be kept until the arrival of the US (schematics in top boxes). The association of CS and US and the subsequent formation of the conditioned response (CR), relies in both paradigms on cerebellar functions, but only the trace demands the contribution of cortex. Due to their conscious and unconscious nature, delay and trace conditioning belong to procedural and declarative learning, respectively (Clark & Squire, 1998). Cortex areas that have been shown to be critical for bridging the memory period for tactile trace eye blink conditioning (TTEBC) in rodents are hippocampus (Tseng et al., 2004), medial prefrontal cortex (mPFC; Siegel* et al.*, 2015) & barrel cortex (BCx; Galvez* et al.*, 2007).*

Eye Blink Conditioning

Eye blink conditioning (EBC) belongs to the classical Pavlovian conditioning paradigms. As such, during EBC a neutral, sensory stimulus is paired with a potent, aversive, stimulus to the eye. The latter is called unconditioned stimulus (US) and is strong enough to elicit an unconditioned response (UR): the eye closure. Typically, a periorbital shock or a corneal air puff serves as US. The neutral stimulus is called conditioned stimulus (CS). It was, so far, of no relevance for the animal, but after learning will be associated with information about the aversive US. During conditioning, the US is presented in temporal sequence with the CS, leading to a premature eye closure upon CS presentation, in order to evade the US. The newly learned behavior is called conditioned response (CR). Two types of conditioning can be differentiated: the delay and trace type.

In the following, I will further elaborate on delay and trace eye blink conditioning. The table in Figure 1 gives a summary on both, highlighting the striking differences in cognitive and neural demands.

Delay eye blink conditioning (DEBC) is characterized by a co-termination of CS and US – despite the misleading term ‘delay’. CS and US overlap in time, but the US starts ‘delayed’, giving the individual a chance to respond to the CS. Since CS and US overlap, the association does not require the CS to be kept in short term memory (Figure 1; left column). Delay conditioning works independently of any awareness about the relationship of CS and US (Clark & Squire, 1998). It is a typical example for **implicit/procedural memory**, which works in **unconscious** ways (as introduced before). Delay conditioned humans, which were tested on blocks of CS-alone and CS-US trials, showed extinction behavior (i.e. fewer CRs) upon consecutive CS-alone presentations, even though they knew, the risk of receiving the next US, increased from trial to trial (Clark *et al.*, 2001). Knowingly, the participants were unable to control their behavior, and adapt the strategy to minimize the number of US to the open eye.

Supporting the dissociation between cognitive contribution and sensorimotor behavior, neuronal lesion experiments have shown that DEBC works perfectly, without cortex (Cx). Removing the whole of Cx (i.e. decerebration) did not affect/impair the acquisition of delay eye blink conditioning (e.g. in rats and cats: Lovick and Zbrozyna, 1975; Norman *et al.*, 1977), and its retention (Mauk & Thompson, 1987). Therefore, Cx is neither necessary for forming the association, nor for the sensory processing of the CS. The neuronal circuitry underlying delay-type association is dependent on the cerebellum (Thompson, 1990; for a review see Woodruff-Pak & Disterhoft, 2008): CS and US are gated, through the pontine nuclei and the inferior olive, respectively, to the cerebellar cortex, where the association is formed and the CR is executed via the cerebellar nuclei. Animals with cerebellar lesions fail to learn and perform DEBC (McCormick *et al.*, 1981; Thompson, 1990).

Trace eye blink conditioning (TEBC) can be derived from the DEBC, by separating CS and US in time such that CS and US periods are non-overlapping, forming the stimulus-free, trace period (Figure 1; right column; Figure 3A). The duration of this period is typically 250-1000ms but can extend up to several seconds. In order to associate the CS with the US, the information about the CS needs to be bridged across the stimulus-free period (e.g. by sustained neuronal activity called a memory 'trace'). Contrary to delay conditioning, TEBC needs the awareness about the relationship of CS and US (in humans; Clark and Squire, 1998). Therefore, trace conditioning is considered a model for the **conscious** recollection of information and is seen as part of the **explicit/declarative** class of **memory**. Unlike in delay conditioning, human subjects, trained on trace conditioning with consecutive series of CS-alone and CS-US pairs, showed CR performances that were highly influenced by their expectation of the next trial (Clark *et al.*, 2001). Here, the CR probability increased with consecutive CS-alone presentations.

The memory trace cannot be generated by the cerebellum, and thus, requires cortical activity (simplified circuitry in Figure 3B). Local lesions or chemical inactivation of medial prefrontal cortex (mPFC), not only hinders the acquisition, but also prevents the performance of TEBC (retention), in mice (Siegel *et al.*, 2015) . Siegel, (2014) found, that mPFC neurons respond to the CS with an elevation of firing rate outlasting the CS presentation. This ramping or persistent activity is the basis of the memory trace, which gets recruited, refined, and strengthened by TEBC training. Interestingly, it is not only the higher association cortices, like mPFC that are critically involved in TEBC. The primary somatosensory area, receiving the CS input from the tactile periphery, turned out to be of major importance for TEBC, in rodents. The model system of choice for TEBC in my study, to deliver a tactile sensory CS, is the whisker system, which I would like to introduce in the next chapter.

The Whisker System

The whisker system imposes as one of the most important sensory systems in rodents (Figure 2). It enables these nocturnal animals to explore their proximal environment and track their way through burrows, even in complete darkness. The tactile organs of the whisker system are the so-called facial vibrissa - the whiskers - on both sides of the animal's snout. Whiskers are organized in a matrix of horizontal rows and vertical arcs, forming the whisker pad (Figure 2; top right blow-up). The rows are labeled alphabetically from A to E, with the A row being the most dorsal row. Each row contains several whiskers, numbered from caudal to frontal. Each whisker ends in a highly innervated hair follicle (Ebara *et al.*, 2002) which can be moved by muscles (Dörfl, 1985) to sweep them actively across objects of interest. This sensorimotor activity, called 'active touch', has many similarities with the similar action employed by humans when actively palpating textured surfaces using their hands or fingertips (Gamzu & Ahissar, 2001).

The tactile information in the hair follicle is taken up by primary afferents, the receptor cells of the tactile system, whose soma is located in the trigeminal ganglion, and which connect to the trigeminal nuclei in the brainstem (1st synapse). From there tactile signals are projected to the contralateral VPM thalamus (2nd synapse), and finally arrive at the primary somatosensory (S1) cortex (3rd synapse), in less than 10ms (Figure 2; green path). Whisker S1 cortex is commonly referred to as 'barrel cortex' (BCx), according to the characteristic and unique, barrel-like patches which appear in layer 4 upon e.g. Nissl staining (Simons and Woolsey, 1979; Figure 2; bottom right blow-up). In mice, each barrel spans an area of ~250µm diameter, equaling the size of a functional, cortical column. These columns, defined by barrel borders are called 'barrel columns'. Strikingly, there is a topological correct 1-to-1 representation of each whisker in one barrel column, such that the barrel cortex map remarkably resembles the spatial organization of the whiskers on the pad.

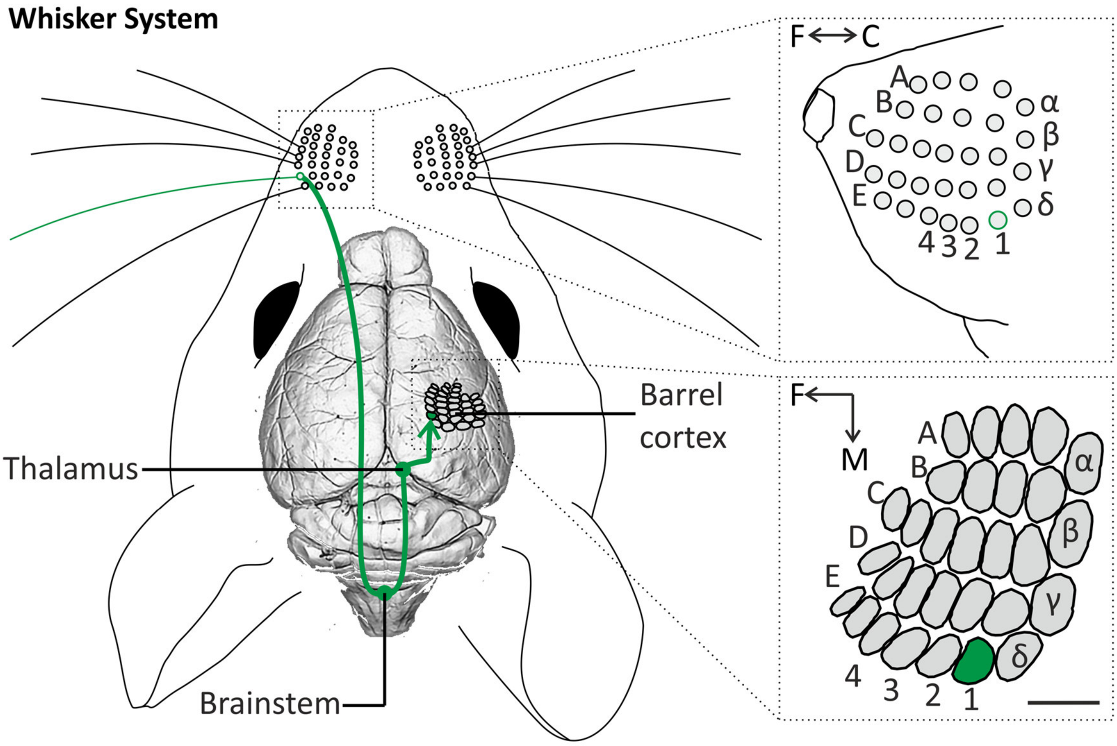

Figure 2 The rodent's whisker system and barrel cortex. *The whiskers are long facial vibrissa on both sides of the snout (organized in rows (letters) and arcs (numbers); top right blow-up), that work as tactile sensors. BCx is the corresponding primary somatosensory area, receiving tactile inputs via brainstem and thalamus (green path) (bottom right blow-up). BCx is characterized by a 1-to1 representation of one whisker in one cortical barrel column, with neighboring whiskers represented in neighboring columns, forming a topographic map (compare both blow-up).*

Each of the mouse' barrel column contains ~10,000 neurons (note, that mouse barrels of smaller whiskers hold less cells (Meyer *et al.*, 2013)). The multitude of columnar neurons are principal excitatory cells (called pyramids), that often project to distant targets. Only 10-15% belong to the versatile group of GABAeric interneurons, providing inhibition onto local neurons. Like, in most other cortical areas, mouse BCx neurons organize in 6 layers. Layer 1

(L1) - the most superficial layer – accommodates mostly axonal and dendritic elements. The ‘supragranular layers’ 2 and 3 (L2/3) extend to a depth of about 300µm. Layer 4 (L4), the ‘granular layer’, extends as far as 500µm and holds the characteristic barrel field in frontal Nissl stainings. The deeper layers 5 (L5) and 6 (L6) reach a depth of 800 and 1000µm, respectively. For an detailed overview on cellular morphologies and organization of BCx see Meyer *et al*. (2013). Beyond 1000µm, we find the white matter (WM) holding almost exclusively axons from cortical afferent and efferent projections.

Within the barrel column, L4 and L6 are the major input layers, receiving the first thalamic input from a tactile stimulus. The afferent signals, however have been reported to directly reach the large L5 pyramids as well (Constantinople & Bruno, 2013). Subsequently, the tactile input undergoes intra-columnar processing, but also spreads to the neighboring barrel columns (Oberlaender *et al.*, 2011; Narayanan *et al.*, 2015). Amongst many columnar connections, we find that L5 neurons receive excitatory synapses from following layers (in decreasing order of magnitude): L2/3, L6 and L5 (autapses). L4 has only few connections onto L5 and L6. Instead, L4 excitatory cells project to themselves and L2/3 (Thomson and Bannister, 2003; for a review see Feldmeyer, 2012).

Adding to the thalamic bottom up input, there are top down projections onto various layers of BCx: e.g. cholinergic (ACh) modulatory input from nucleus basalis/basal nucleus (L1; Kristt, 1979; Buzsaki *et al*., 1988), S2 secondary somatosensory cortex (L2/3 L5 & L6; DeNardo *et al*., 2015); other primary sensory areas (L2/3 & L5; Miller and Vogt, 1984). All those inputs offer options to modulate BCx activity (and induce plastic changes), thus affecting intra- and/or intercolumnar computations.

Major S1 BCx output layers are L5 and – to a lesser extend - L3 & L6. BCx in general has direct cortical connections to whisker related M1 and S2 (Koralek *et al.*, 1990; Chakrabarti & Alloway, 2006). Subcortical projections depart mostly from L5 (thick tufted pyramidal cells). Apart from feeding back to thalamus, they target brainstem, the reticular formation, tectum, basal ganglia, and the cerebellum (Bosman *et al.*, 2011).

The whisker system has been examined extensively, providing a model system to study sensory processing and sensorimotor control. Amongst several advantages, the classic and well-established head fixed preparations for awake behaving rodents (Schwarz *et al.*, 2010; Guo *et al.*, 2014b), grants easy access to the vibrissa for precise stimulus presentation, and also otherwise offers high experimental accessibility and control. Furthermore, the well-known neuronal connectivity (within and outside BCx), the topographic BCx layout and the easy to access location on top of cortex, favors BCx as a structure to study cortical functions. In fact, BCx has been subject to various tactile TEBC studies reporting structural and functional changes during learning, creating a profound basis for the current study.

The Whisker Barrel Cortex in Tactile Trace Eye Blink Conditioning (TTEBC)

As mentioned above, the delay form of eye blink conditioning does not require somatosensory cortex. In this case, tactile processing and perception of the CS is not mediated through BCx. In contrast, a BCx lesion blocks the acquisition of trace conditioning, in rabbits (Galvez *et al.*, 2007) and mice (Galvez *et al.,* 2011). Furthermore, Galvez *et al*. (2007) found a significant reduction in CRs after BCx lesions in trained animals, suggesting that 'an aspect of the trace association may reside in Bx'. Their data, however, show a quick return to the pre-lesion performance within a few retraining sessions.

The acquisition of TTEBC does not only require BCx function, but also induces various, task dependent, plastic changes. Galvez *et al*. (2006 & 2011) discovered TTEBC dependent map plasticity, in rabbits and mice. They showed, that barrels in L4, receiving the CS expanded in trace conditioned but not delay conditioned mice. The expansion goes along with a structural plasticity in the same layer. L4 excitatory neurons gain spines during TTEBC training, with the level of spin gain being correlated with the number of CRs (Chau *et al.*, 2014). This formation of new synapses complies with current concepts of learning a new stimulus association, while a recent study showed, that BCx also loses spines. Joachimsthaler *et al*. (2015) trained mice on TTEBC, while monitoring the apical tuft in L1 of L5 thick tufted pyramidal cells. Dendrites inside (but not outside) the conditioned barrel column lose up to 22% of their spines. Despite those findings, the role of BCx during TTEBC is still elusive. The redundancy of BCx during DEBC, and its importance during TTEBC, together with the plastic changes, suggest a role that goes beyond simple tactile processing.

Aim of the study

BCx is required for trace (but not delay) eye blink conditioning, while learning induces BCx map and spine plasticity. In the present study I ask, whether there are signals in BCx in trace interval, which have the potential to bridge the temporal gap between CS & US? Furthermore, the question arises, if (and how) BCx activity is modified by conditioning? I sought to answer these questions by investigating laminar LFP and spiking activity in BCx, during tactile trace eye blink conditioning in mice. I used current source density (CSD) and multi-unit (MU) analysis in naïve and conditioned animals to explore the electrophysiological/neural effects of TTEBC training. The CSD, is a method to analyze multi-channel LFPs. Based on evoked laminar multi-electrode recordings, the CSD indicates the locations of net transmembrane currents, that enter and leave neurons (and neuronal networks) as current sinks and sources, i.e. neural network activation.

So far, there is no report about the ability of rodents to generalize TTEBC from the trained to other whiskers. Although, previous studies suggested that mice and rats generalize to adjacent (i.e. directly neighboring), but not far whiskers in a fear conditioning (Gdalyahu *et al.*, 2012), and a gap-crossing (Harris *et al.*, 1999) paradigm, respectively, it is still unclear, whether they do so in TTEBC. I tested the ability of mice to generalize from the trained whisker to adjacent, near and distant whiskers.

Finally, I was interested whether the BCx signal found in these experiments maybe causal for TTEBC acquisition? I used the optogenetic toolbox for temporally precise perturbation of BCx. Shining light on the Cx of the well-established optogenetic VGAT-ChR2-eYFP mouse line (Zhao *et al.*, 2011; Guo *et al.*, 2014a) induces the activation (i.e. action potential firing) of all inhibitory GABAergic interneurons, which in turn silences excitatory neurons. To address the afore mentioned questions, if signals during CS or trace are causal for TTEBC, I optogenetically blocked BCx activity in the VGAT mice, during CS & trace or trace period alone, during conditioning.

A previous study suggested, that BCx activity is as well essential for TTEBC performance (Galvez *et al.*, 2007). Nonetheless, the shown performances just drop slightly after BCx lesions. To revisit the question, whether BCx activity is necessary for TTEBC performance (retention), I blocked BCx specifically during CS & trace periods in trained animals.

Material & Methods

The experimental and surgical procedures were conducted in agreement with German animal law and approved by the local authorities.

Animals. Adult, male wild type **C57BL/6N** and **VGAT-ChR2-eYFP** (Schematics in Figure 4D; Zhao *et al*., 2011) mice were used in this study. The VGAT-ChR2-eYFP mouse line is an optogenetic tool that can be used for area specific and highly time-resolved Cx perturbation. The genetic modification leads to the expression of the optogenetic product channelrhodopsin-2 (ChR2) and the yellow fluorescent protein (eYFP) exclusively in GABAergic neurons. Activating the ChR2 leads to a mixed ion current, depolarizing the neuron which in turn inhibits many neurons in its surrounding (Figure 4D). The sum effect from many inhibitory cells is that an entire column of cortex can be silenced. After surgery all animals were housed separately on an inverted 12h day/12h night cycle with food and water *ad libitum*.

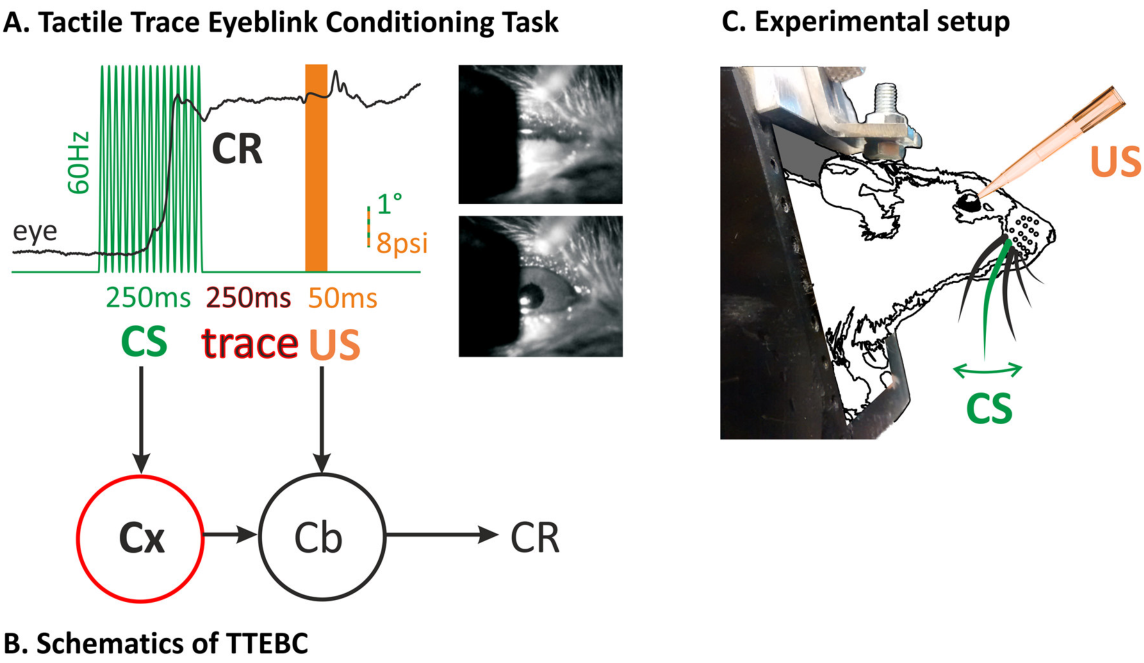
A. Tactile Trace Eyeblink Conditioning Task

C. Experimental setup

B. Schematics of TTEBC

Figure 3. Behavioral paradigm and setup. (A) *Tactile trace eye blink conditioning (TTECT) requires to keep CS signals (250ms, 5°, 60Hz, sinusoidal; green line) in memory during the 'trace' period (here 250ms) in order to associate them with the US (50ms, 40psi, orange bar) and respond with an eye closure as a conditioned response (CR; black line; eye closure is illustrated by the video stand-stills on the right).* ***(B)*** *TTEBC requires the interplay of cortical areas (Cx), like BCx, and cerebellum (Cb).* ***(C)*** *Mice learned TTEBC in 5 daily sessions (5x60 CS-trace-US-pairings) using a single whisker CS, a corneal air puff US, and a head fixed preparation (Schwarz* et al.*, 2010).*

Surgical procedure. All chronic implantations were performed under 3 component fentanyl anesthesia, containing fentanyl (Ratiopharm GmbH, Germany), midazolam (Hameln pharma plus GmbH, Germany) and medetomidine (Sedator®; Eurovet Animal Health B.V., Netherlands).Anesthesia was initialized by *i.p.* injection of 0.05mg/kg fentanyl, 5mg/kg midazolam, and 0.5mg/kg medetomidine, and maintained by one third of the initial dose, administered every 1-2h. Throughout the whole surgery, eyes were kept moist by a moisturizing ointment (Bepanthen® Augen- und Nasensalbe; Bayer AG, Germany).

After skin opening, the scull was scrapped clean and remaining adhesive tissue was removed with 3% hydrogen peroxide solution ($H_2 0_2$; Wasserstoffperoxid Lösung 3% Ph.Eur.; Otto Fischar GmbH & Co. KG, Germany). Subsequently, the scull was coated with a light curing bond (Optibond™ FL; Kerr GmbH, Germany) and a thin layer of dental cement (Tetric® Evoflow; IvoclarVivadent AG, Liechtenstein), sparing the trepanation sites. A trepanation of ~3x3mm was drilled, -2mm frontal and 4mm lateral to bregma on the right hemisphere, above the barrel field, leaving the dura mater intact. To identify the barrel map, intrinsic optical imaging (see below) was performed on the E1 and surrounding whiskers (Figure 4A). All E1 barrels of wild type and VGAT-ChR2-eYFP mice were implanted with electrodes or a light fiber, respectively (see below). In case of electrode implantation, 2 silver ball electrodes were placed on the cerebellum, serving as ground and recording reference. After fastening the implants with dental cement, a 10 mm, M3 screw was attached for experimental head fixation. At the end of surgery, the anesthetic agents were antagonized, using a *s.c.* bolus of 1.2mg/kg Naloxone (Hameln pharma plus GmbH, Germany), 0.5mg/kg Flumazenile (Frisenius Kabi GmbH, Germany) and 2.5mg/kg Atipam (Eurovet Animal Health B.V., Netherlands).

As post-surgical treatment the animals received analgesic medication (Carprofen; Rimadyl®; Zoetis, UK) and antibiotics (Baytril®; Bayer AG, Germany) for the following 2 and 7 days, respectively.

Intrinsic optical imaging is a non-invasive method to map evoked neuronal responses in the intact neocortex. Intrinsic optical imaging utilizes the effect, that the light spectrum being adsorbed by neuronal tissue changes with the amount of local blood flow, which, in turn, is tightly coupled to neuronal activation (Grinvald *et al.*, 1986). The repetitive, 60Hz, E1 whisker deflection, induces strong activation of the stimulated E1 barrel column, which is revealed under red light illumination as change in the hemodynamic signal (Figure 4A left panel; barrel border was derived by thresholding). By mapping at least two or more surround whiskers (e.g. D1, C1 & δ), I created a part of the topographic barrel map, verifying the location of the E1 barrel. The right panel of Figure 4A shows some barrel columns mapped on the surface of the cortex aligned by the surface blood vessels.

Experiments. All animals were trained on **tactile trace eye blink conditioning (TTEBC)** using the following CS, trace and US parameters. For the **CS**, a supra-threshold, 5°, 60Hz sinewave, tactile stimulus was applied to the E1 whisker for 250ms (Figure 3C; green line). For this purpose, the whisker was threaded into a 100µm hole of a 10mm long, custom made arm,

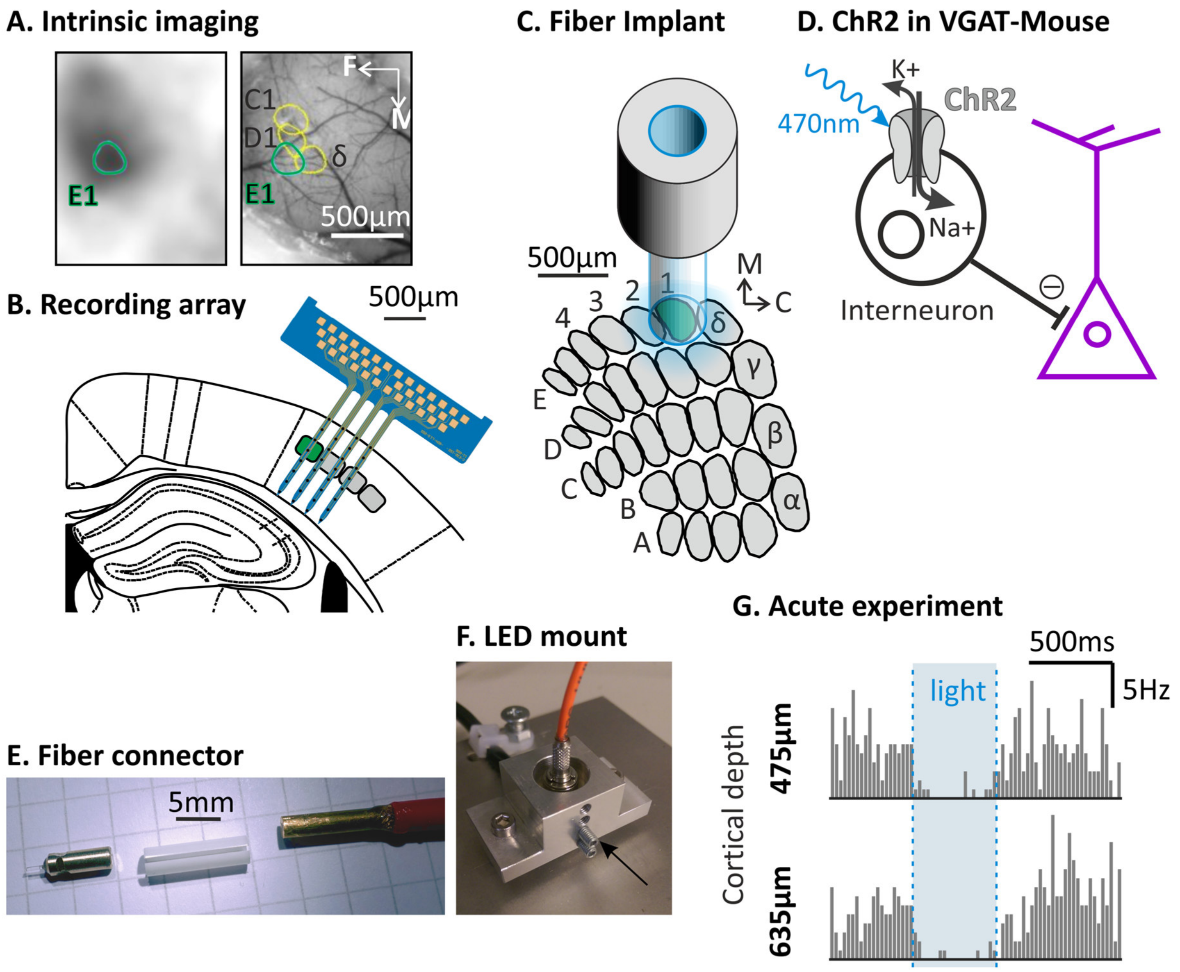
A. Intrinsic imaging
E1
F
M
C1
D1
δ
E1
500µm
B. Recording array
500µm
C. Fiber Implant
500µm
4
3
2
1
M
C
δ
γ
β
α
E
D
C
B
A
D. ChR2 in VGAT-Mouse
K+
470nm
ChR2
Na+
⊖
Interneuron
E. Fiber connector
5mm
F. LED mount
G. Acute experiment
500ms
5Hz
light
Cortical depth
475µm
635µm

Figure 4. Physiological methods. (A) *Intrinsic optical imaging to map receptive fields during surgical implantation. The hemodynamic signal indicates the cortical location of the principle barrel column of a stimulated whisker (E1; left panel). Adjacent whiskers are represented in neighboring columns, superimposed on the cortical surface blood vessel system (D1, C1 and δ; right panel),* ***(B)*** *Four-shanked, 32 channel silicone probe placed in the barrel field to record local field potentials (LFP) and multi-unit (MU) activity from the principle, adjacent and near barrel columns (maximal distance two column widths).* ***(C)*** *Fiber implant placed at the cortical surface of the principle barrel column (E1). Blue light was applied to activate channelrhodopsin2 (ChR2) expressed in inhibitory interneurons.* ***(D)*** *Mechanism of cortical silencing in the VGAT-ChR2-eYFP mouse line* (Zhao *et al.*, 2011). *The optogenetic activation of ChR2 with blue light (470nm) leads to a depolarization of interneurons (black), and a subsequent, feed forward, GABA mediated hyperpolarization, i.e. inhibition of pyramidal cells (purple).* ***(E)*** *Fiber implant. A 400µm glass fiber glued into a custom made, 2.5mm alloy ferule served as chronic fiber implant (left). The implant is tightly connected to a 1.5m light fiber (right; orange) by a ceramic mating sleeve (middle), creating a stable light connection.* ***(F)*** *Custom build LED mount holding a 470nm high power LED (hidden underneath the fiber block; black arrow) served as light source. The light is coupled into an 800µm light fiber (orange) with the fiber block allowing all degrees of freedom for placing the blunt fiber tip at the LED.* ***(G)*** *Preliminary experiments under anesthesia to verify the efficacy of optogenetic BCx perturbation in the VGAT-ChR2-eYFP mouse line. The bar blots show trial averaged spiking activity (bin size: 25ms) at cortical depths of 475 and 635µm of 500ms, Shining 4.3mW blue light (blue patch) on the cortical surface silences the example neurons.*

attached to a galvanometer (6210H Galvanometer Scanner & analog servo driver 677XX; Cambridge Technology; Bedford, MA USA) that was placed 5mm from the whisker pad. For easier insertion into the stimulator, the whisker tip was trimmed, and to avoid inadvertent stimulation, some of the surround whiskers were shortened, one week prior to training. Following the CS, the stimulus free **trace** period was chosen to be 250ms – matching most other previous TTEBC experiments, for better comparison. A corneal air puff served as **US** consisting of a 50ms air blow applied to the cornea via a thin 200µl pipette tip at 40psi and a distance of ~3mm. The strength of the air puff was chosen to securely evoke a complete eye closure.

For experimental training I used the well-established head fixed preparation, providing highest stimulus and experimental control (Schwarz *et al.*, 2010). Figure 3C shows a head fixed mouse inside one of our custom build restrainer boxes. All animals were thoroughly handled and subsequently habituated to head fixation, for 2 weeks prior to the experiments. During TTEBC training mice received 300 CS-trace-US pairings, spaced by a random inter trial interval (ITI) of 20-40s. Training was performed over 5 sessions on 5 consecutive days, with 60 trials, each.

To mask any possible acoustic emission by the tactile stimulator, a 60dB white noise was present at all time.

Eye blink performance. Eye blinks were recorded at 2kHz, throughout the training, using an IR light source and sensor (OPR5005; Optek; Carrollton, TX, USA), being placed in proximity to the eye, to which the US was applied (Weiss & Disterhoft, 2009). Any eye closure effects the amount of reflected IR light, causing a voltage change on the sensor. As previously tested by Joachimsthaler *et al*. (2015), a change in voltage output relates linearly to the size of the eye closure: Δ0.4mm eye closure results in 1V sensor change. For TTEBC I picked the following criteria for a conditioned response: (1) 260ms after CS onset (i.e. 10ms after CS offset), the eye closure has to exceed 5 times the standard deviation (and at least 0,2V) of its 500ms baseline period (measured just before the CS onset). (2) This eye closure needs to be maintained throughout the trace period, until US onset. An example CR trace is shown in Figure 3A.

To minimize trials with strong blinking or the eye closed prior to CS onset, the last 500ms of each ITI was analyzed online, during TTEBC. In this period, every eye closure that exceeded the maximum UR amplitude minus 0.8 mm, postponed the next trial by an extra ITI, randomly picked from an interval of 2-4s.

I separated trials with conditioned responses (abbreviated by CR) and no conditioned responses (nCR), calculating the session performance, as percent of CR (Figures 5A & 9A; 13C-E). Animal performance during the first vs. last 60 trials was termed **naïve** vs. **expert** performance. In order to control for eye movements, the first and last trials in which the animals did not generate an eye blink (nCR) were called nCR(naïve) and nCR(expert) respectively (Figure 8).

Electrophysiological implants. Three wild type C57BL/6N mice were chronically implanted with 32-channel, 4-shank silicone probes (E32-150-S4-L2-200; Ø 35 µm Pt; tips sharpened; 30mm cable assembly; Omnetics® connector; Atlas Neuroengineering bvba, Belgium, Figure 4B) to record extracellular, neuronal activity during TTEBC acquisition. Each of the 4 80x50µm shanks, being spaced by 200µm (total range: 600µm), carries 8 low-impedance, 35µm platinum electrodes with an inter-electrode spacing of 150µm (total range: 1050µm). The silicone probes were implanted in BCx at a depth of ~1050µm, spanning all cortical layers. The 4 shanks were oriented across barrel rows and along the barrel arc, so that the first shank was centered in the previously identified, E1 barrel column, and the 4th shank sat in C1. (Figure 4B)).

Electrophysiological recordings Electrophysiological data was continuously collected at 20kHz sampling rate, during TTEBC training, in mice with silicone probe implants. The silicone probes were connected through a custom adapter with four 8-ch head stages (MPA8I; Multi Channel Systems GmbH; Germany), pre-amplifying the signal in proximity to the head of the mouse. The signal was subsequently channeled to the signal collector (SC8x8; Multi Channel Systems GmbH; Germany), broad band filtered from 1-5000Hz and 500x amplified by a filter amplifier (FA64I; Multi Channel Systems GmbH; Germany), and finally acquired by a 128ch recording system (ME128-PGA-MPA-Syste; Multi Channel Systems GmbH; Germany).

LFP/CSD analysis. The LFP signal was derived from the raw recordings, by down-sampling to 2kHz, and <200Hz low-pass filtering (3rdorder Butterworth filter; Figure 6B). All 32 channels could be successfully recorded in two animals, while in animal B the most superficial channel of the distal shank had to be excluded in animal B, as it was strongly contaminated by humming noise. The matrix of LFP signals was converted into a current source density map (Nicholson & Freeman, 1975; Mitzdorf, 1985).

The **current source density (CSD)** analysis uses the second spatial derivative of the LFP recordings to derive information about relative current sources and sinks in the recorded in extracellular space. It thus reports where and when currents enter or exit the system. Here, a negative CSD, is called a 'sink' and is due to positively charged ions entering a cellular compartment (exit the extracellular space) or negatively charged ions leaving the cell (entering the extracellular space). The exact origin of sources and sinks in any CSD analysis is complex and a sum of different types of current flow in and out of diverse cellular compartments. A typical contribution to sinks is thought to be (1) presynaptic activity (positively charged ion flow, like Ca++, into the terminal) or (2) postsynaptic excitation (positively charged ion flow like Na+, into dendrites and somas). Sinks on the other hand can be reflections of non-active sites on dendrites (return currents via leak channels) or inhibitory postsynaptic effects (negatively charged ions like Cl- flowing inside the cell).

In the present study I used the kernel based current source density method (kCSD; Potworowski *et al*., 2012), which provides the CSD measure in space (the electrode plane), across trial and session time (for each TTEBC trial individually).

For further analysis, this 4-dimensional CSD map was averaged across certain trials (e.g. naïve vs. expert trials) to yield trial averaged 3-dimensional maps. In a first approach, these were then split into 4 separate data sets holding the 2-dimensional CSD across cortical depth and time for each electrode shank (Figures 7A/C, 8A-C & 9B/D). A different cutout of the trial averaged CSD map yielded the lateral current spread across the shanks, for the following 10 time points (in ms after CS onset): 0, 6, 8, 10, 12.5, 15, 20, 25, 100 and 300 (Figure 7D). Through this dissertation, current sinks are coded blue, sources are red, and white stands for zero current.

To compare the LFP signal in naïve and expert mice, I assessed the distribution of CSD values across trials in each space-time bin and calculated the area under the receiver operator characteristics curve (AUC). In statistics AUC is a common non-parametric measure of effect size with values between 0 and 1 with 0.5 marking random performance and 0 and 1 indicating perfect discriminability (Green and Swets, 1966; Figure 7A middle row, Figure 8A-C bottom row). In order to test, whether an AUC value deviates significantly from 0.5 (no effect), 95% confidence intervals (CI) were obtained by comparing bootstrapped distributions (random classification from the total sample of CSD values obtained in one space-time bin (1000x; areas of significant CSD changes during learning are indicated by black lines on AUC maps)

Spike analysis. To extract spikes from the electrophysiological recordings, a reference channel was picked and subtracted from all other 31 raw signals; to reduce common/global noise. Hereafter, the data was high pass filtered, using a zero-phase 3rd order Butterworth filter with a cut off frequency of 500Hz. Spike timestamps and multi-unit wave forms (MU) were derived by thresholding and wavelet analysis. Single-unit analysis was not pursued as stability of single-units across may well be possible, but cannot be guaranteed, and are therefore difficult to defend. For spike extraction, all parameters were kept constant within a recording channel, across recording sessions, to allow comparison between naïve and expert spiking rates. To identify a possible rundown effect of the electrodes, I compared spike rates in the 500ms baseline window, prior to each CS, and MU amplitudes for naïve and expert electrode channels (Figure 11A & B).

MU spiking activity is expressed as firing rate in Figures 10, 12A & Appendix 1-4 (1ms bin size; forward filtered by 10ms boxcar) and averaged for naïve and expert eye blink conditioning trials. All MUs were tested on their ability to code for/detect the CS by a change in firing rate (Figure 11C). I classified a MU to code for the CS, whenever its firing rate during the 250ms CS period was significantly different from the 500ms pre-CS, baseline period. I assessed the effect size of CS responsive MUs for each shank individually [by means of an AUC analysis with 1000 bootstrap iterations] in naïve and expert trials. AUC values >0.5 vs. <0.5 characterize MUs, with elevated vs. depressed firing rates, respectively, during the CS period.

Based on MU response properties I further subdivided a TTEBC trial into fast CS onset response from 4-15ms, CS persistent response from 50-250ms, and the trace activity from 300-500ms. Subtracting the baseline firing rate from each of these windows, enabled me to directly compare their naïve with expert MU activity, as effect sizes. Training effects on MU firing rates were derived by AUC analysis with 1000 bootstrap iterations. The data was split, either by distance from the principal barrel or columnar depth (in reference to the two prominent CSD sinks in L4 and L5/6).

The Appendix Figures 1-4 show each individual MU, including TTEBC training effects for all significant changes in firing rates for CS onset, CS persistent, and trace period, and naïve and expert PSHTs and wave forms (±sd).

Generalization Paradigm. Four mice were tested on their ability to generalize from the trained E1 whisker to other whiskers. The test whiskers, were an adjacent **D1 or δ** whisker, the near **C1** whisker, or the far **α** whisker (Figure 13A). During extra post-training sessions, every 6th conditioning trial was replaced by the test CS (5°; 60Hz sinewave; 250ms) to one of these untrained whiskers. The test stimulus, was never paired with a US, to avoid new conditioning; and each whisker was tested in one session, containing 10 test trials. The tests were performed sequentially from far whiskers to neighboring ones to assess generalization behavior. Test eye blink trajectories were normalized to the median of trained whiskers trials, within each session, for quantitative comparison of eye blink responses to test, and to trained whisker stimulation. The data was subsequently pooled in adjacent, near and far whiskers, and the median response variability computed as interquartile range (IQR, i.e. range from the 25th to the 75th percentile).

Fiber implants and optogenetic experiments VGAT-ChR-eYFP mice were chronically implanted with fiber implants, to shine light on the surface of the BCx during TTEBC. The implant was assembled of a short piece of 400µm light fiber (0.39NA, FT400UMT; Thorlabs GmbH, Germany) and a custom made alloy ferrule (either new silver or bronze) with an outer diameter of 2.5mm and a length of ~7mm (Figure 4E; left). The fiber was glued into the ferrule with epoxy resin, so that the side pointing towards the brain, stuck out by around 3mm. Both sides of the fiber implant were grinded thoroughly, to maximize light input and output. The fiber implant was placed and fastened, directly on the cortical surface, straight above the E1 barrel (Figure 4C).

In some preliminary experiments the effectiveness of optogenetic BCx perturbation was tested. The initial surgical methods and anesthesia were the same as described above for the chronic implantations. After the trepanation, a high-impedance (>3MΩ) glass-electrode was lowered into BCx, recording single spiking units at various cortical depths. A 400µm light fiber was placed on the Cx surface, above the spot of the electrode position, through which a constant 4.3mW light pulse of 500ms duration was applied 50 times at 0.2Hz.

In optogenetic experiments with fiber-implanted animals a **470nm** blue high-power LED (NCSB119 32lm with PCB; Nichia Corporation, Japan), mounted on a custom made aluminum holder served as the light source for the optogenetic experiments (Figure 2F; the black arrow indicates the position of the LED). The light was fed into an 800µm fiber (0.39NA, FT800UMT; Thorlabs GmbH, Germany) which was in turn, coupled to the 400µm fiber implant by a 2.5mm, ceramic mating sleeve (Figure 4E), creating a very tight, stable and reproducible fiber connection. The LED was controlled by a LED driver (LEDD1B; Thorlabs GmbH, Germany) generating a continuous light pulse of **4.3mW** output intensity at the cortex surface. This intensity was at least 3-fold higher than the one, needed to efficiently suppress excitatory spiking throughout all cortical layers, in awake mice (Guo *et al.*, 2014a). To minimize rebound firing at the light offset (Guo *et al.*, 2014a), each pulse was tapered out over the course of 500ms. To avoid entrainment of additional frequencies, which might serve as CS, I used a constant, non-pulsatile light, that was found to be highly efficient at ChR2 activation in the preliminary experiments under anesthesia.

In the present study, three different experimental paradigms examined the effect of optogenetic perturbation in both TTEBC acquisition and performance. In the first experiment, animals were trained on eye blink conditioning (5x60 trials), adding optogenetic light to the CS, trace & US periods. Light onset was picked to be 10ms prior to CS onset, ensuring that optogenetic perturbation was completely established upon CS presentation. The second set of animals received optogenetic light during trace & US period. Light onset was hereby picked to be 20ms after CS offset, leaving the percept of the whole CS untouched. The third optogenetic experiment was conducted on previously trained, expert mice. Here, TTEBC performance was examined over the course of 5 training sessions (i.e. 5x60 trials), using CS, trace & US optogenetic light.

A 470nm LED house light was installed close to the mouse and lit during the experiment, to mask possible light scattering from the optogenetic stimulus.

Software. Experimental control and data analysis was done, using Matlab® (V2014b; The MathWorks, Inc.). Intrinsic optical imaging was operated by HelioScan V3.1.0 (Langer *et al.*, 2013). The intrinsic images were analyzed in ImageJ. MU spike extraction was conducted through the wavelet, Matlab-plugin Waveclus (Quiroga *et al.*, 2004).

Results

I trained head fixed, male mice on a tactile trace eye blink conditioning paradigm, using a 250ms, 5°, sinusoidal, tactile CS, applied to the E1 whisker, a 250ms stimulus free trace interval and a 50ms corneal air puff (Joachimsthaler *et al.*, 2015; Figure 3A & C). Head fixation, described in Schwarz *et al*. (2010), allowed a high experimental control: precise presentation of CS and US, and the optimal monitoring of the eye closure.

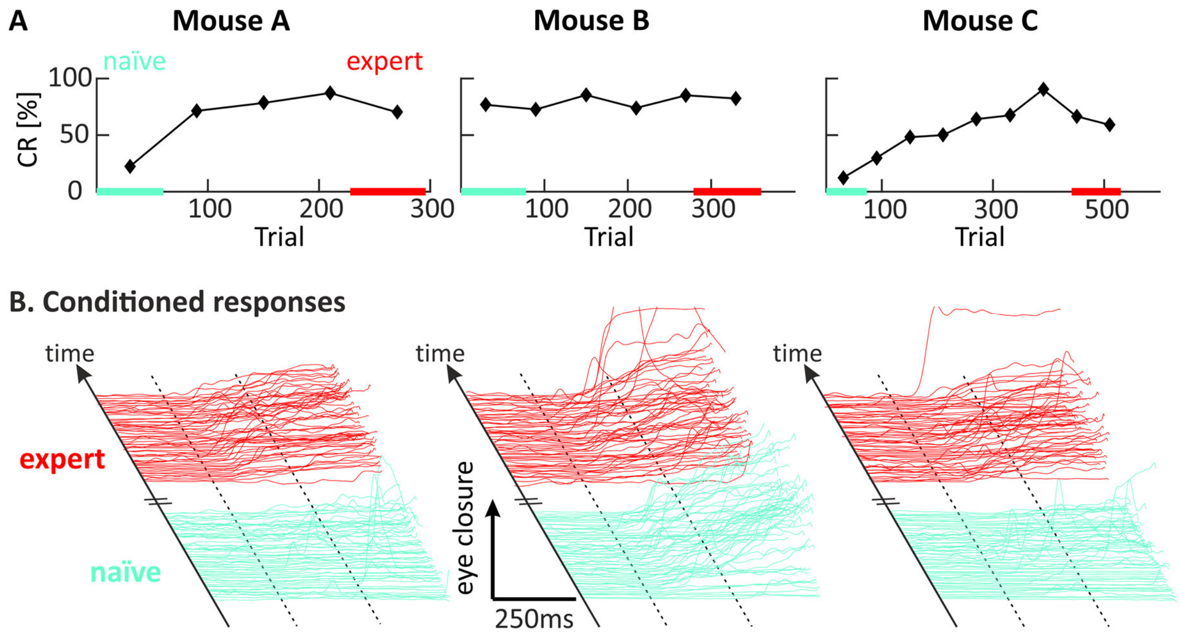

Figure 5. Eye blink psychophysics. (A) *Learning curves of three mice, that were electrophysiologically recorded (cf. Fig. 6-12), plotted as percent conditioned responses (CR). Colored bars indicate the first (naïve; turquoise) and the last (expert; red) 60 trials that were used for further analysis.* ***(B)*** *Eye closure trajectories plotted as waterfall plots for the afore-mentioned trails. Broken lines mark CS on- and offset.*

The three wild type mice used for electrophysiology all learned the CR, closure of the eye upon CS presentation (for details how a conditioned response was defined, see eye blink performance in material and methods; example CR in Figure 3A), within 300 CS – trace – US pairings over the course of 5 days. The fastest learner amongst the three mice showed the first CR after the 5th pairing (Mouse B; Figure 6A & B; middle panel). As observed before, the CRs were variable amongst (but not within) animals (Joachimsthaler *et al.*, 2015). Nonetheless, common features of CRs are that they start around 70ms after CS onset, and at first do not close the eye completely. During the CS & trace period the eye closure becomes more and more complete. Sometimes full closure is only reached with the reflexive eye closure occurring after US presentation. (Figures 3A, 5B, 14A & B). All animals reached a criterion performance of >50% CRs (Figure 5A). In comparison, as shown in an earlier study, pseudo-conditioned animals reach spurious CRs levels <20% (Joachimsthaler *et al.*, 2015).

A. Electrode placemement

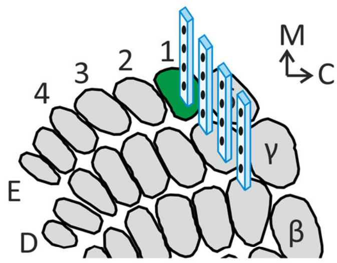

B. Average LFP response (AnimalB)

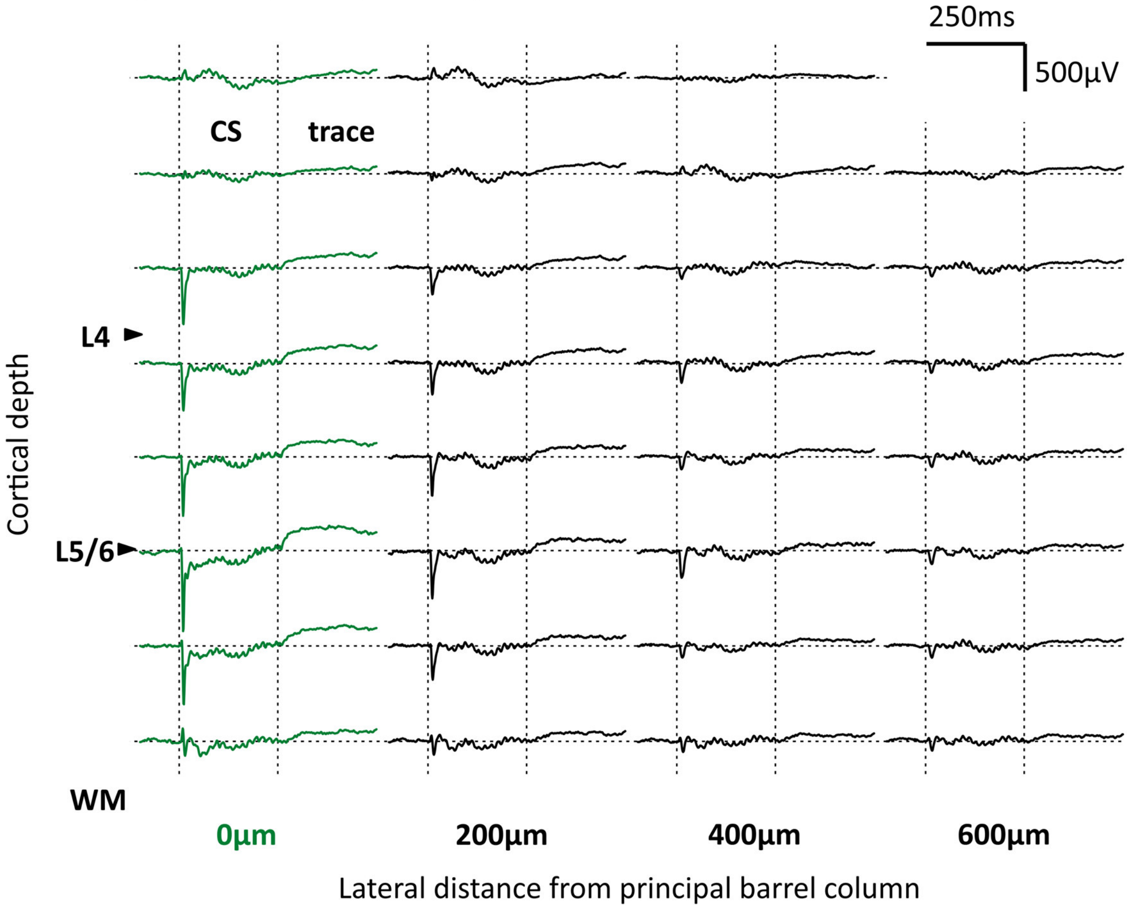

Figure 6. Electrophysiology. (A) *32 channel Silicone probe were used to record LFP and MU activity from the principle (E1), adjacent (D1) and near (C1) barrel columns.* ***(B)*** *Raw LFP response (<200Hz) to CS (vertical broken lines) across the principle shank (0µm; green) and neighboring shanks at lateral distances of 200-600µm, averaged for the first 60 TTEBC trials of animal B. The cortical depth of each recording is indicated by the landmarks: layer 4 (L4), boarder between layer 5 & 6 (L5/6), and white matter (WM).*

Neuronal activity during TTEBC

To characterize neuronal changes during TTEBC, I recorded extracellular signals from BCx in 3 wild type mice. All three mice reached a performance of >50% CRs during the 2nd, 1st and 3rd session, respectively (Figure 5A). In the expert state all animals show ample numbers of characteristic CR trajectories, as they start to close their eye upon CS presentation (Figure 5B; bottom panels).

Four-shank silicone probes were used that held a 4x8 matrix of recording points with inter-electrode distances of 150µm in the vertical and 200µm in the horizontal direction. The four shanks straddled the barrel columns E1 to C1 (Figure 6A) Thus, three barrels, one principal (E1) and two adjacent ones (D1, C1) were monitored. Two types of recordings, LFP and unit data were assessed, converted into CSD maps and MU spike trains, and compared in the naïve and expert state of the animal (first and last 60 trials).

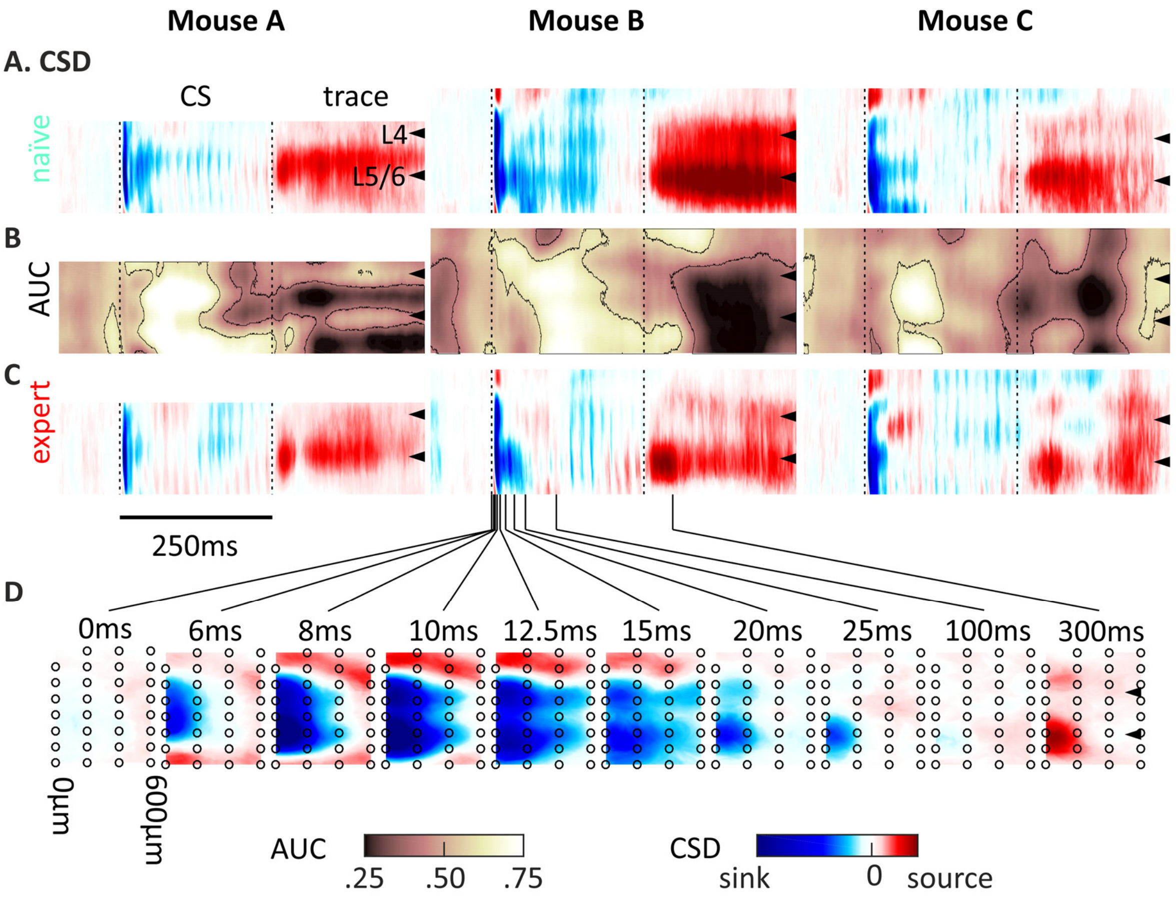

Figure 7. Principal column current source density (CSD) analysis. (A) *CSD across the principle shank for the three mice in the naïve phase. Sink to source range of CSD maps for animal A, B & C: -0.8 to 0.32, -0.5 to 0.2, & -0.4 to 0,16.* ***(B)*** *TTEBC training effect size as area under the receiver operator curve (AUC); p<0.05 significance is highlighted by black-brimmed areas). Cortical layers L4 & L5/6 are marked by black triangles.* ***(C)*** *same as A but for expert mice.* ***(D)*** *Lateral spread of the expert CSD activity for Mouse B at varying time points. Black circles: electrode positions.*

The LFP comprises information about a population of neurons around the electrode (Kajikawa & Schroeder, 2011; Lindén *et al.*, 2011; Leski *et al.*, 2013). Figure 6B shows an example of a matrix recording of evoked LFP trial-averaged within the naïve phase (first 60 trials; mouse B). The evoked LFP recorded from the principle barrel was characterized by peaks corresponding to the spike response ~10ms after stimulus onset (1st broken vertical line; Simons, 1978; Hentschke *et al*., 2006). The peaks were predominantly negative with a maximum close to the thalamus recipient layers L4 and L5/6 and reverted to a positive peak only close to the pial surface as reported earlier (Jones & Barth, 1999) likely corresponding to layer 2. This fast onset response was followed by weaker, persistent activity, displaying small but clearly visible 60Hz oscillations (matching the CS sinusoid frequency). After CS offset (2nd broken vertical line), i.e. in the trace period, the signal consistently assumed positive potentials. The positive potential was maximal at the border of L5/6, the same depth at which the onset response assumed its extreme, but did not reverse across the recorded depth. It is therefore likely that the synaptic origin of the trace activity is different from the one of the fast response. Evoked potentials in CS & trace period were attenuated across shanks but were readily visible at small amplitude across the entire recording matrix, i.e. as far as the secondary adjacent barrel column C1 (600µm).

Next, the LFP matrix was converted into CSD maps (Figure 7; source red, zero current density white, and sinks blue). CSD maps obtained from the first shank (principal barrel column) in naïve and expert mice are shown in panel A and C, respectively. Panel D depicts the lateral spread of CSD across shanks at different points in time after CS onset (mouse B). The absolute CSD amplitudes were observed to vary between mice (mouse A: -0.80 to 0.32, mouse B: -0.50 to 0.20, and mouse C: -0.40 to 0.16 [sink to source]), but the maps scaled to the CSD extremes obtained from the three animals revealed that the spatiotemporal patterns were very similar (Figure 7A, columns). (In animal A, the silicon probe was implanted too deep in the cortex thus that the two deepest electrodes reached into white matter and gave a flat LFP/CSD signals. The data from this animal are therefore depicted as a 6x4 matrix).

Confirming earlier results (Swadlow *et al.*, 2002) the CSD maps were characterized by strong short latency sinks (~8ms after CS onset). Following the strong onset response, which distributes with a few milliseconds across most of the depth of the barrel column, I observed a far weaker sink spreading across layers but with a clear peak at the border of layer 5/6. This response was marked by ripples at 60 Hz corresponding to the CS frequency. Interestingly, centered at the same depth (border L5/6), a clear source developed after CS offset and remained visible throughout the trace phase. The CSD reveals the different reversal of the fast onset response (~layer 2) and the tonic response throughout the trace period.

These general characteristics were seen in the naïve and expert phase (Figure 7A & C). Nevertheless, quantitative comparison of the CSD maps in naïve and expert using the AUC effects size, revealed clear and consistent differences (Figure 7B). The general direction of changes was toward zero current density such that both, the sink in the CS period and the source in the trace period, were diminished. These changes, however, showed statistically significant patterns that were consistent across the three mice. Changes exceeding the 95% prediction interval obtained by bootstrapping (encircled in by a black line in Figure 7B) were observed across infragranular layers late in the CS and throughout the trace period. It is important to stress that, in contrast to the persistent CS and trace responses, the CSD responses evoked at short latency were stable during acquisition of conditioned eye blinks in all three mice.

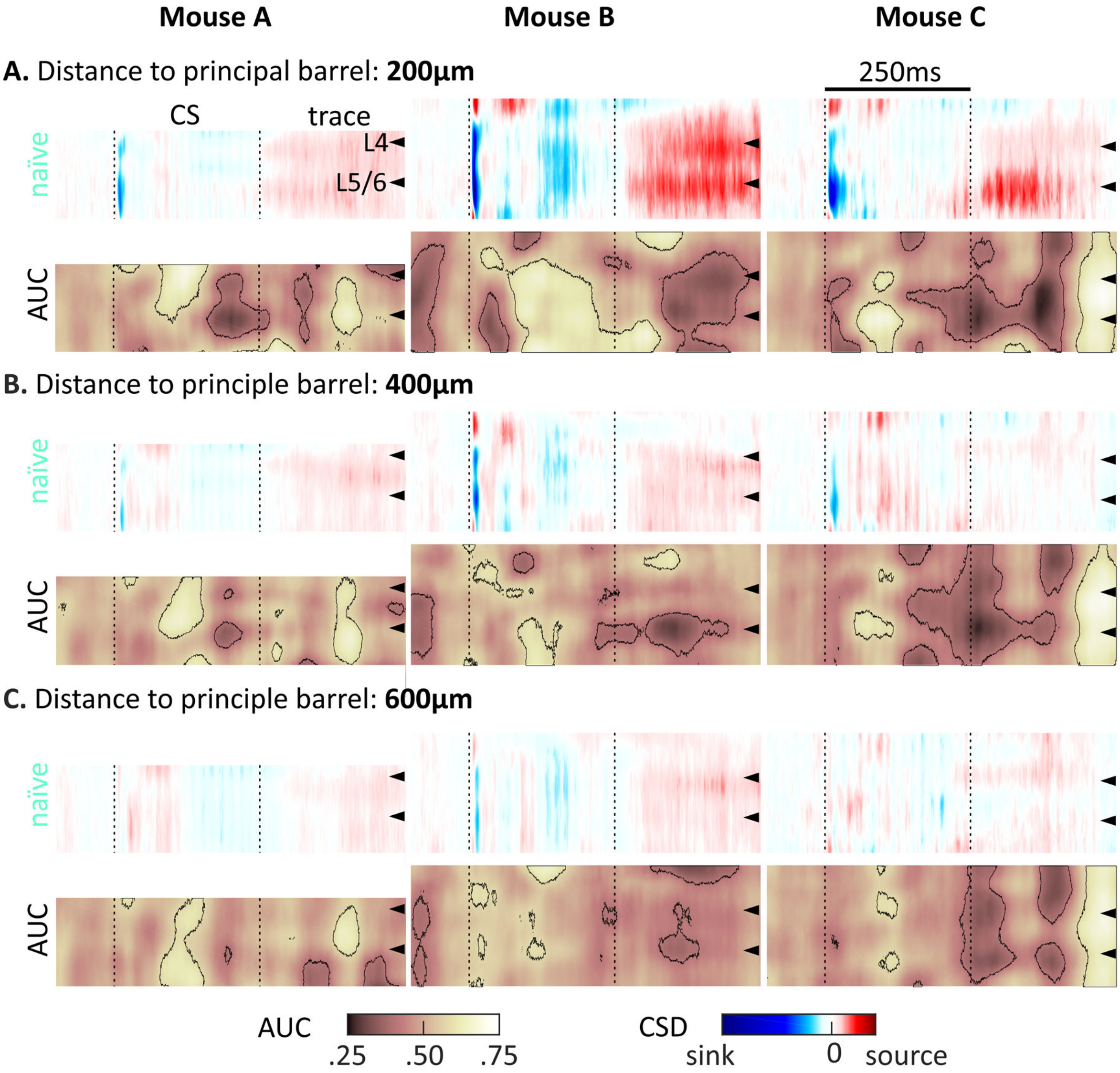

Figure 8. Adjacent and near columns CSD analysis. (A-C) *CSD analysis as in Fig. 7, across the 3 shanks at distances of 200-600µm from the principle barrel column (CSDs of expert mice are omitted). Same conventions as in Figure 7.*

The lateral spread of CSD activity is shown for a series of peristimulus times in figure 7D. Again there were clear differences between the fast onset sink(s) and the continuous source during the trace period. The fast sinks clearly spread to the adjacent barrel columns, while the source during trace period was largely bound by the principal barrel. Also, again, the different reversal locations were prominently visible in these plots. These phenomena can be appreciated as well in the CSD-time plots of the 3 remaining shanks off the center of the principle barrel (Figure 8). Here in addition, it is revealed that the CSD attenuation during learning continues to be present outside the principle barrel column.

Motor Signals and Movement Artifacts

All previously analyzed naïve and expert trials were chosen irrespectively of whether the mouse performed a CR or not, and thus, electrophysiological recordings might be contaminated with motor signals and movement artifacts. Different degrees of lid movement in expert vs. naïve states could be sufficient to make up the found training effect in the CSD analysis. To control for this possibility, I analyzed only trials, in which the mouse failed to perform a conditioned response (nCR), i.e. the CSD and AUC analysis presented in Figure 7 was repeated using exclusively nCR trials. A problem with mouse B was that it learned so quickly that the two classes overlapped in time. In fact, mouse B generated only 50 nCR trials in total. Therefore, in this case 25 nCR naïve trials were compared with 25 nCR expert trials (colored ticks in Figure 9A). In mouse A and C, naïve and expert nCR trials were found in separated training session. The CSD maps obtained from the nCR trials contained all aspects discussed earlier for naïve and expert mice (Figure 9B-D), most clearly in mice A and C. The CSD map were largely the same as seen before, and also the general attenuation of CSD during learning was present. Mouse B did not show the effect as nicely, presumably due to the wide distribution of naïve and expert nCR trials. Nevertheless, the attenuation of CSD activity late in the CS period is readily observed as AUC effect size (Figure 9C). In summary, I conclude that

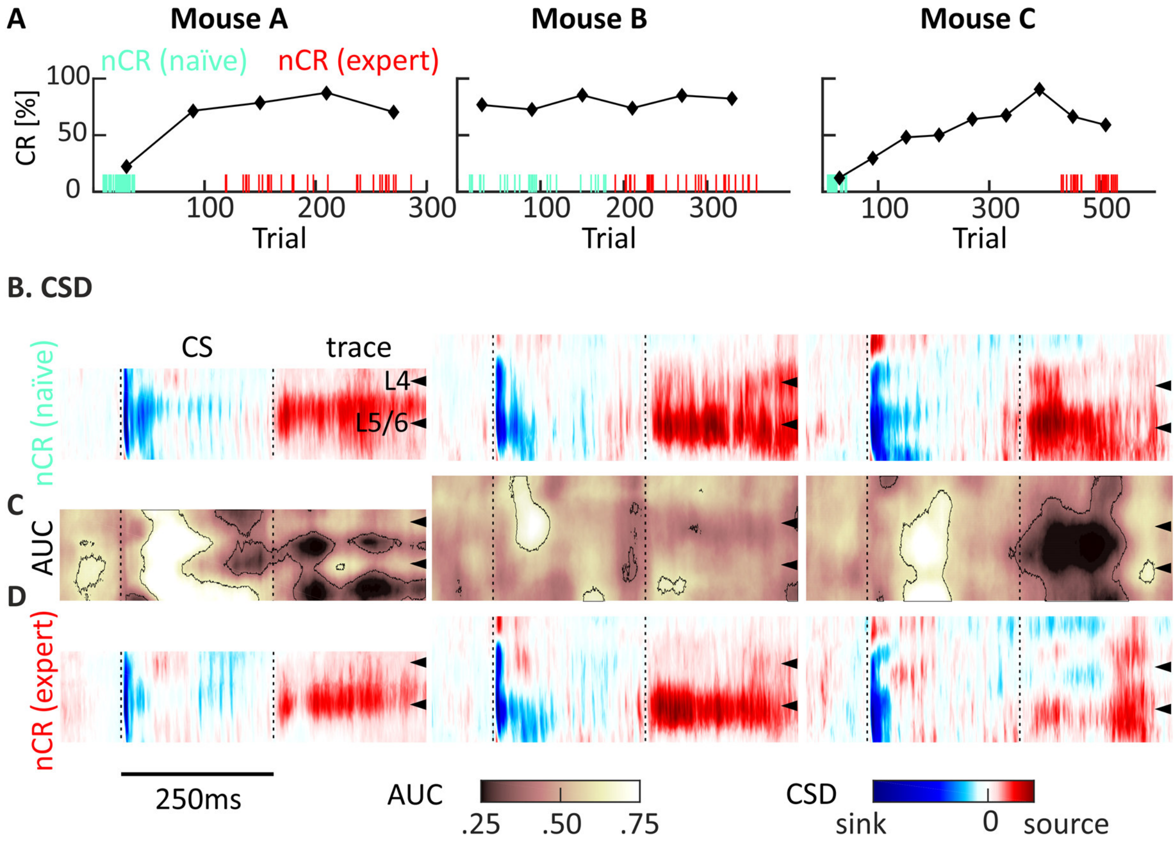

Figure 9. CSD analysis exclusively for not responded (nCR) trials. (A) *Same data as in figure 5A. The colored ticks indicate the naïve (nCR naïve; turquoise) and expert (nCR expert; red) nCR trials.* ***(B-D)*** *As in figure 7A-C, but now plotted exclusively for nCR trials.*

the patterns and changes of CSD maps described earlier (cf. Figure 7) are due to learning rather than movement production

Spiking and MU activity

Next I was interested, how spike data would reflect the CSD patterns and learning related changes. Multi-unit spiking activity (MU) was found in all channels (electrodes). As unit recordings cannot be expected to be perfectly stable across 5 days we refrained from trying to isolate single unit data: all extracted units were classified to be of the MU type. To compare firing rates obtained in naïve and expert trials the baseline firing rate (obtained in a window of 500ms before CS onset in all cases) was subtracted. The comparisons were done for the first 60 naïve and the last 60 expert eye blink training trials for each of the three animals (as done for CSD maps in figure 7). Statistical comparison of MU firing rates was estimated by AUC and significance of change was assumed if it exceeded the 95% prediction interval derived from a bootstrap procedure (x1000). The stability of the spike recording during the 5 days of training was demonstrated by an only slightly increasing background firing (within a 500ms period before CS onset; naïve 30.8Hz±27.8sd vs expert 39.3Hz±25.6sd; Wilcoxon rank sum test: p=0.008), stable spike amplitudes (naïve 66.1µV ±19.2sd vs. expert 65.1µV±16.2; Wilcoxon rank sum test: p=0.94) and stable CS onset responses, that, as would be expected from the classic literature, decay with increasing distance to the principal barrel column (Simons, 1978), but were stable across the training sessions (color, Figure 10).

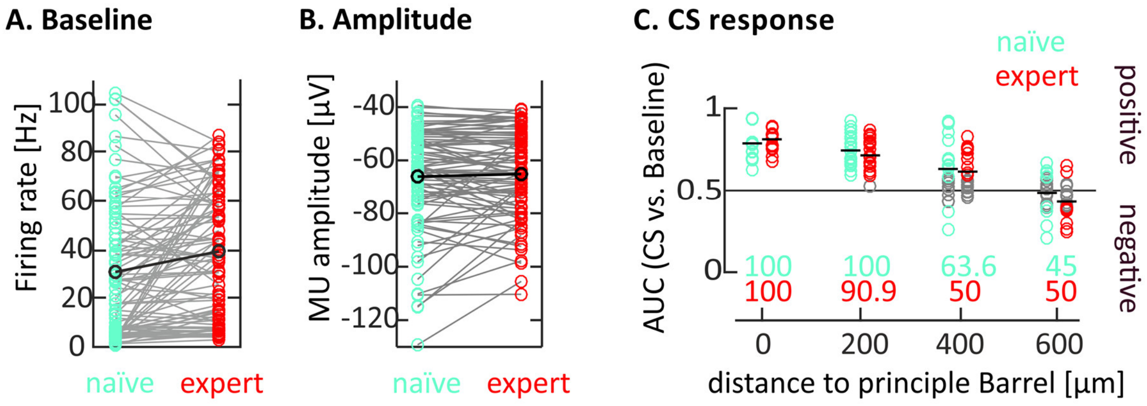

A. Baseline

B. Amplitude

C. CS response

Figure 10. Multi-unit (MU) baseline activity and CS response*. *(A) *500ms, pre-CS baseline firing rates for all MUs in naïve (turquoise; mean: 30.8Hz±27.8sd) & expert (red; mean: 39.3Hz±25.6sd; Wilcoxon rank sum test: p=0.008) animals.* ***(B)*** *MU spike amplitudes in naïve (-66.1µV±19.2sd) and expert (-65.1µV±16.2sd; Wilcoxon rank sum test: p=0.94) mice.* ***(C)*** *AUC for MU responses to CS presentation in naïve vs. expert trials (Colored circles indicate significant effects; p<0.05; bootstrapping), split by electrode shank. Colored numbers indicate percentage of MUs responding to the CS.*

Figure 11 shows the detailed firing rates measured in the principal barrel column (1st shank of silicon-array) for naïve and expert trials (colors) in all three mice. As introduced in previous figures, the CS onset and offset is marked by broken vertical lines. The cortical layers, as assessed from CSD maps, are marked as well. All MU firing rates show a sudden increase at CS onset at a latency of ~8ms, which then quickly relaxed to reach a lower persistent response throughout the CS period. In the trace period many MUs showed firing rates that were somewhat lower than the baseline. Firing rate changes were highly specific in peristimulus time and direction. In summary, while baseline and excitatory onset response were stable (cf. Figure 10), the persistent CS & trace response changed in decreasing directions.

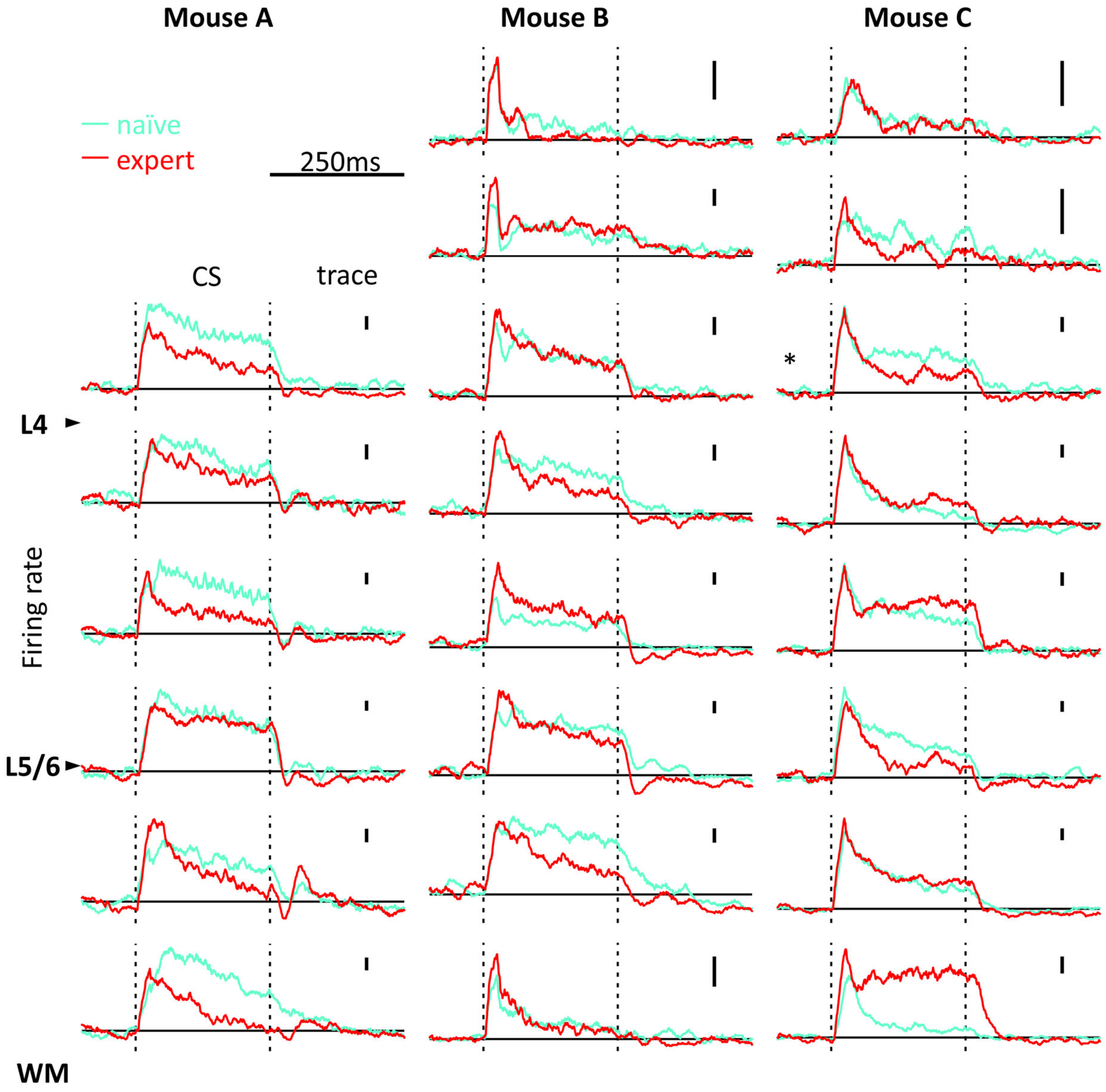

Figure 11. MU activity in the principle barrel. *Naïve (turquoise) & expert (red) PSTHs (normalized to baseline) across the principle barrel column in the three mice. Broken lines: CS on- and offset. Cortical layers L4 & L5/6 are marked by black triangles. Scale bars: 50Hz. Asterisk marks a recording with the typical decrement in expert persistent-CS and trace firing rates.*

The detailed analysis and statistical appraisal of these effects are provided in Figure 12. The firing rate was measured in three time windows ‘CS onset’, ‘CS persistent’, and ‘trace period’ (indicated in Figure 12A as green, yellow and orange bars), matching the three different response phases of the LFP (4-15ms after CS onset as the fast thalamic CS response; 50-250ms ongoing/persistent response; and 300-500ms trace activity). The firing rate of a typical MU is shown again in panel A, with typical learning-related decrease visible in CS persistent and trace periods. Panels B and C summarize the MU population effects across horizontal distance (B) and cortical depth (C). All MUs with significant training effects in either of the time windows, are highlighted by color (non-significant changes, gray). The numbers in panel B detail the fraction of significant positive (AUC >0.5; top) and negative (AUC<0.5; bottom) effects. The CS onset response was unaffected in the majority of the MUs with an overall average AUC value close to 0.5 (black lines). The most distant MUs at 600µm show a negative tendency, but response strengths there are very low. In contrast, task acquisition was paralleled by a significant reduction in the persistent CS & trace period. The majority of neurons shows a significant negative effect size across all shanks, suggesting that response changes during learning are not confined to a single barrel column (Figure 12B). Plotting the same effect sizes across the depth of recording (for all shanks) the main negative effects in persistent CS & trace phases show no obvious variation along cortical depth. The CS onset response is generally not affected by learning – a negative effect in the two most superficial electrodes cannot be

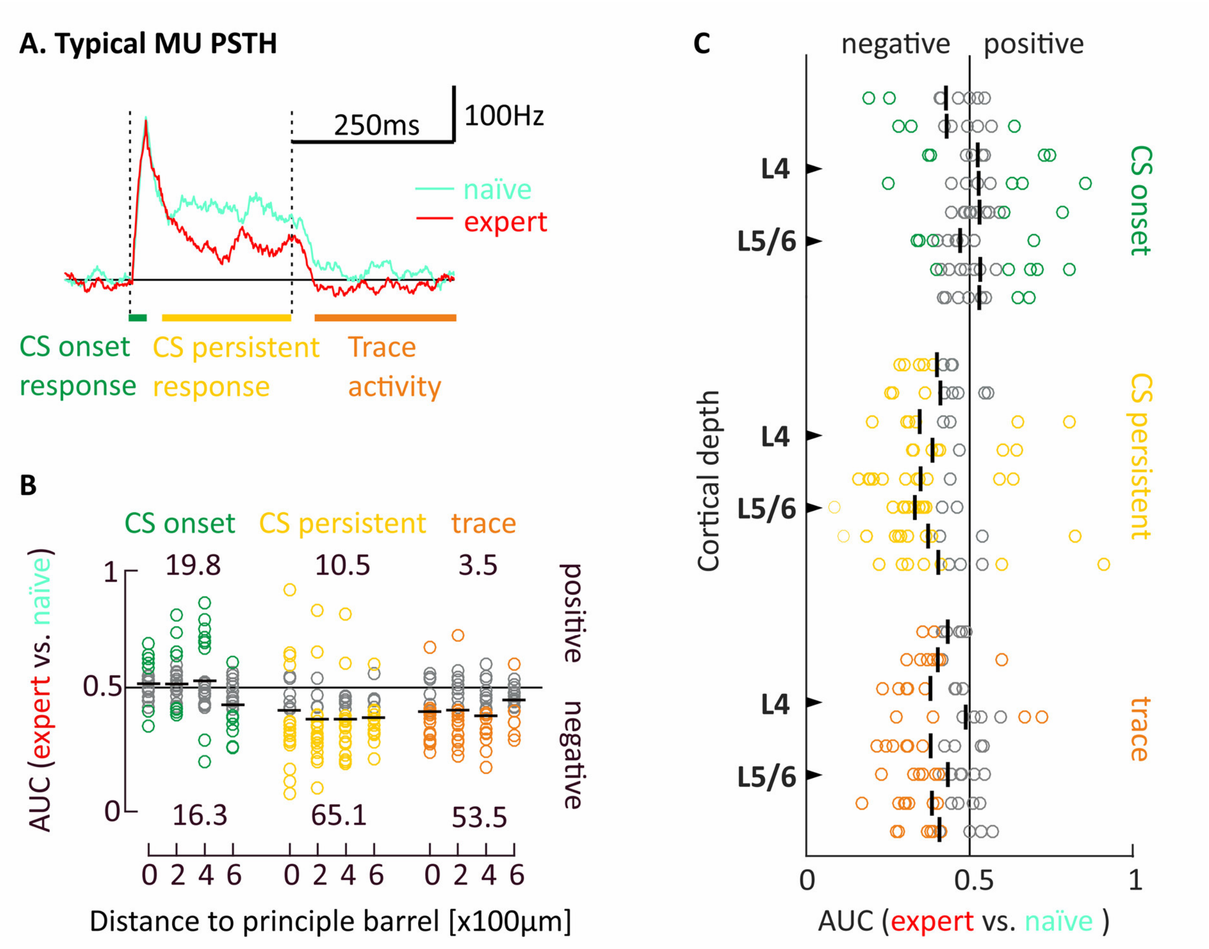

Figure 12. Firing rate changes during TTEBC. (A) *Example PSTH (cf. marked by an asterisk in Fig. 11). The colored bars indicate the periods analyzed in B and C.* ***(B and C)*** *AUC of naïve vs. expert trials in the three peristimulus time periods (marked in A): 4-15ms CS onset (green); 50-200ms CS persistent; and 300-500ms trace. Colored circles indicate significant AUC effects; p<0.05; bootstrapping. Black lines indicate the mean.* ***(B)*** *AUC along the horizontal cortical axis at distances of 0-600µm from the principal barrel column. Numbers: percentage of MUs that are positively/negatively modulated.* ***(C)*** *AUC throughout cortical depth. Cortical layers L4 & L5/6 are marked by black triangles.*

excluded, although it seems to be driven by outliers. The total sample of MU PSTHs can be found in the Appendix (Figure A1-A4), including all significant AUC values, given as color coded bars underneath the respective PSTH segment.

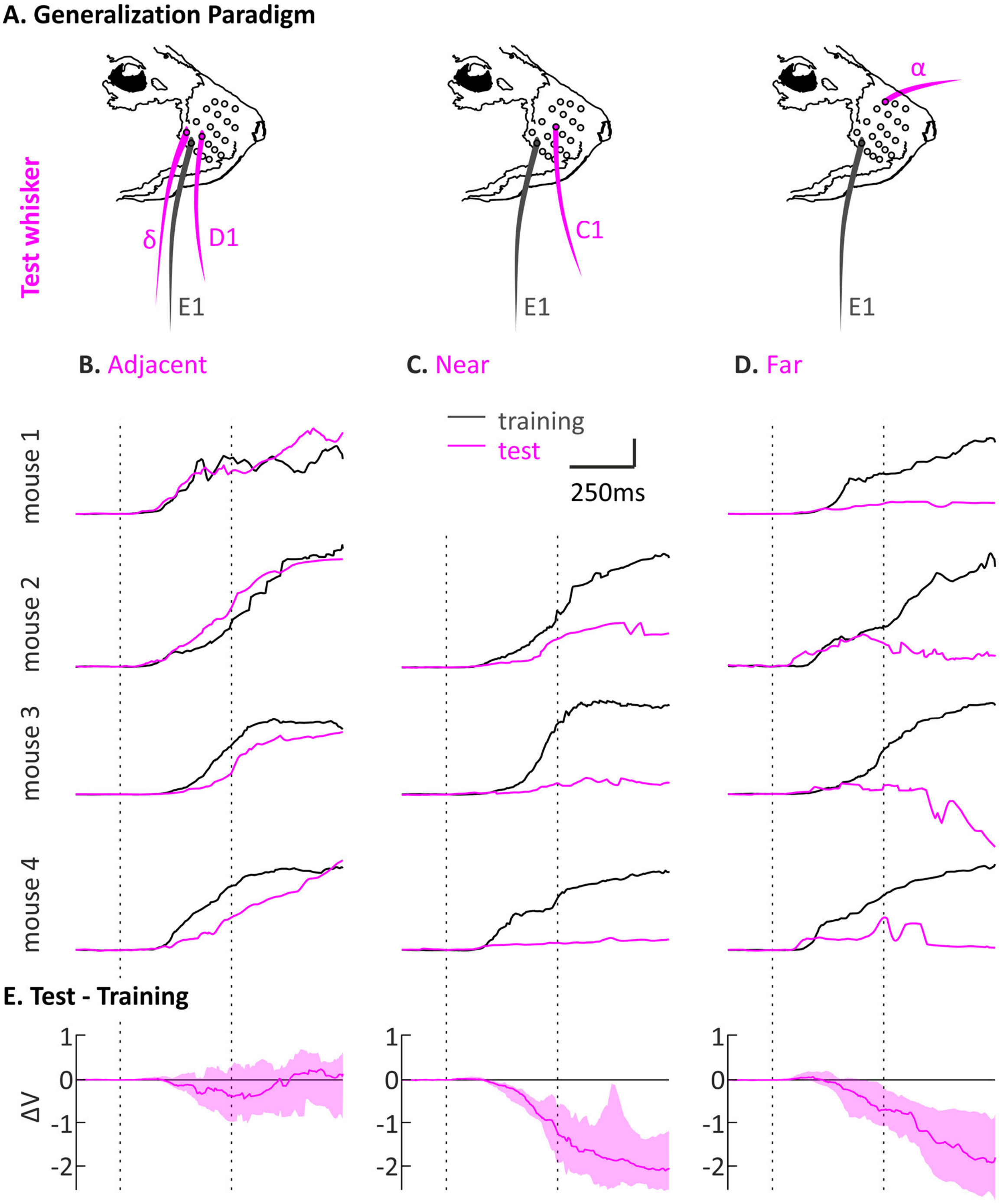

Figure 13. ***Generalization to neighboring whiskers in TTEBC. (A)*** *Mice were tested on their ability to generalize the trained E1 whisker (grey) association to adjacent (D1 or δ), near (C1) and far (α) whiskers (pink),* ***(B-D)*** *Median eye blink trajectories in response to E1 (trained whisker; grey) and test whisker (pink) in four mice. Broken lines indicate CS on- and offset. Note, that the test whisker CS was never paired with the US.* ***(E)*** *Difference in eye blink trajectories of test and trained whisker as delta V (ΔV), pooled across four mice for each generalization step. Median eye closure differences at the end of the trace period (line) and interquartile ranges (IQR, pink patch): Adjacent: 0.1V (IQR 1.4); Near: -2.0V (IQR 1.3); Far: -1.7V (IQR 1.9).*

In summary, the spike analysis confirms the temporal specificity of findings in the CSD analysis. Acquisition of TTEBC training is accompanied by specific suppression of MU activity in the CS persistent and trace periods. Spatially the effect in spiking is more widespread as compared to CSD. It is most prevalent in the principal and directly neighboring barrel column, but occurs equally in all layers.

Generalization to other whiskers

Responses and their learning-related changes found here (CSD and spiking), as well as plastic changes described in a previous study (spines, Joachimsthaler *et al.*, 2015) were confined to the principal barrel column and its direct neighbors. I, therefore, aimed to find a behavioral reflection of this specificity. To this end I tested the ability of mice trained on TTEBC using a single whisker CS to behaviorally generalize to other whiskers (Figure 13). Together with the whisker used for training (E1), I chose to investigate the eyelid response to the following untrained 'test' whiskers: 'adjacent' (**D1 or δ**), 'near' (**C1**; one interjacent barrel column), and 'far' (**α**) (Figure 13A). Four mice, fully trained on the E1 whisker (300 trials, 5 days) were tested in additional post learning sessions in the following way: In each session, I delivered ten CS to either of the test whiskers (never followed by an US), randomly intermingled with fifty regular CS-US pairings using trained whisker E1. The first post-learning session started with the far whisker, followed by the near whisker. Adjacent whiskers were tested last. Comparison of session-averaged eye lid trajectories (Figure 13B-D) revealed that adjacent CS evoked an identical CR as the trained whisker, while full generalization of the CR failed to reach farther. Near and far CS' evoked a slower and aborted eyelid movement as compared to E1 and adjacent whiskers (Figure 12C; mouse 1 was not tested on C1). Typically, the eye closure during the CS had a much smaller amplitude (near whisker: median max V trained 2.3(IQR 1.8) vs test 0.5(IQR 1.2); Wilcox-test: $p=5E-9$; far: max V trained 2.9(IQR 1.7) vs test 1.2(IQR 2.4); Wilcox-test: $p=3E-5$) and often led to an opening of the eye again within the trace period, as if the mice realized that it is the incorrect stimulus (ΔV 500ms after CS onset, at the end of the trace period, just before the US: Adjacent 0.1V (IQR 1.4); Near: -2.0V (IQR 1.3); Far: -1.7V (IQR 1.9); Figure 13E). Importantly, such deviating movements did not happen in the regular CS-US trials. In summary the extend of full CR generalization reflects well the mentioned confinement of functional and morphological plastic changes to the principal and adjacent barrel columns.

Optogenetic Perturbation of BCx during TTEBC.

So far I demonstrated, that BCx is activated in persistent CS & trace period during acquisition of TTEBC, and that this activity is specific to the barrel column receiving the CS and it immediate neighbors, matching the range of CS generalization in mice. The next question was, whether BCx activity is causally related to TTEBC learning. We already know that BCx lesions prevent TTEBC learning (Galvez *et al.*, 2007; Galvez *et al.*, 2011), i.e. BCx clearly has an instructive effect on TTEBC learning. However, it is not clear whether this critical role is assumed by barrel cortex' CS or trace activity, or both. Results from chronic lesions are not helpful to decide this question. I therefore resorted to optogenetic blockade of BCx which can be targeted in a temporally specific way to one of these trial periods. I used the VGAT-ChR2-eYFP mouse line, which upon blue illumination shuts down the activity of an entire column (Figure 4). I implanted these mice with light fiber placed on the surface of the trained principle barrel column (E1). While training these mice on the TTEBC, constant 470nm blue light with a

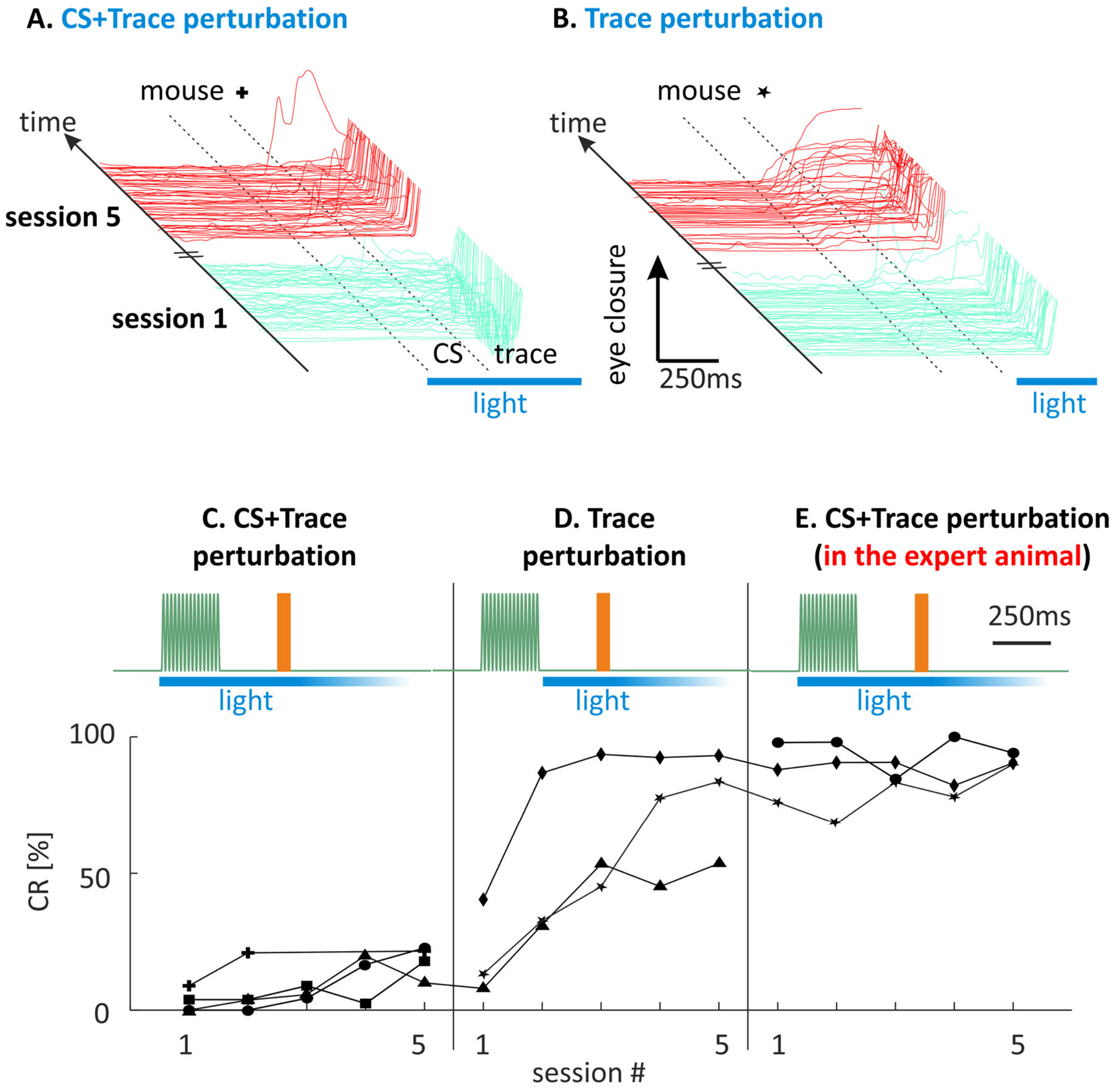

***Figure 14. Optogenetic BCx blockade during TTEBC acquisition and retention**. Eye blink trajectories under optogenetic BCx blockade of CS & trace **(A)** or trace-only **(B)** periods (blue bars) during the acquisition of TTEBC for the 1st (turquoise) and 5th session (red), in 2 example mice ✚ and ✶. Broken lines: CS on- & offset. **(C,D)** Learning curves as percent CRs of individual animals in the two afore mentioned experiments. **(E)** Performance curves of individual expert mice (i.e. TTEBC retention) during CS & trace BCx blockade. Conventions of CS and US iconic plots as in figure 3 and blue bars as in panels A and B.*

total intensity of 4.3mW was shone on the principle barrel column, during the ‘CS + Trace’ period or the ‘Trace’ period alone. Figure 14A & B shows example eye blink trajectories of the first (turquoise) and the last (fifth; red) training session - under the two illumination patterns. Mouse ✚ received CS+trace blockade and failed to learn the task. The CR ratios (number of CR divided by number of trials) for session 1 and 5 were 8.9% and 21,6%. These numbers do not exceed those of pseudo conditioned animals as reported earlier (Joachimsthaler *et al.*, 2015). Thus, perturbation of CS & trace period effectively prevented the mouse from learning the TTEBC paradigm, which supports the results from chronic lesions. Mouse ✶, in contrast, received Trace BCx blockade, making CS activity available for learning TTEBC. This mouse readily acquired the task with a CR ratio of 83,9%. The results obtained with all mice are plotted in figure 14C & D. I trained four animals on the CS+trace paradigm, and three mice on the Trace paradigm. One of the four CS+trace mice then learned the task without optogenetic interference and was retested again using CS+trace while expressing the learned task (i.e. retention). Two of the mice which learned the task under the Trace condition were subjected to the CS+trace condition while expressing the learned behavior. None of the three mice tested in the retention phase showed signs of losing the learned behavior with blockade of BCx. Together these results clearly indicate that only CS activity assumes a critical role for TTEBC acquisition, while the activity in the trace period is non-critical for learning. In contrast, retention of learned content is independent of BCx function (confirming earlier experiments using lesions; Galvez *et al.*, 2007).

Optogenetic activation of GABAergic, inhibitory interneurons could lead to, either blocking of spontaneous BCx activity, or activation of GABAergic projection neurons, which might be both perceived by an animal, and hence serve as a CS. Post experimentally, all VGAT mice received optogenetic-only trials (i.e. no tactile whisker CS), to test, whether the optogenetics perturbation was used as a CS. Surprisingly, I identified about half of the animals to show CRs to light onset, even when the tactile CS was absent. Mice that could use light as the CS were excluded from the experiment, prior to the analysis. The data set presented in Figure 14 originates exclusively from mice that did not show CRs to light stimuli alone, and thus failed to use light alone as a CS.

Discussion

My study shows that the acquisition of TTEBC leads to a suppression of BCx spike activity during CS persistent and trace periods, mirrored by a respective decrement of local CSD intensity. Matching the lateral spread of activity into neighboring barrels, I find that mice show generalized associations only to adjacent (but not near or far) whiskers. Finally, I show, that the acquisition of TTEBC requires BCx activity during the CS but not during the trace period. After five days of training, the retention of TTEBC performance is independent of BCx activity.

BCx role for TTEBC acquisition and consolidation

I show that BCx CS activity is critical for acquisition but not for retention. The principle of this functional reorganization is known already from lesion studies (Galvez *et al.*, 2011), but had been never specified for the CS vs. trace period. My optogenetic blockade has the advantage over lesions that it excludes the possibility that plastic changes are triggered by function loss that harness other brain structures to take over lost functionality. The dispensability of BCx for retention shown with lesions in the earlier studies could have been due to such restorative plastic changes. However, my optogenetic blockade, excluding such lesion-triggered plastic changes, fails to suppress TTEBC memory in early retention, too. Therefore, plastic changes triggered by learning (not by the blockade!) must be the underlying mechanism. This finding sits well with the common view that multiple mechanisms on the systems level underpin memory consolidation (Zola-Morgan & Squire, 1990; Kim & Fanselow, 1992). Generally, it is assumed that hippocampal-cortical circuits contribute to acquire memories in the first place, and then lead to the second phase of early memory consolidation (‘recent memory’), lasting up to four weeks, in which the memory is maintained by a spreading array of cortical areas with hippocampal contribution fading out. In a third phase of late consolidation (‘remote memory’), after a few weeks, memory is hippocampus-independent and held by a pruned set of core cortical nodes (Grosso *et al.*, 2015). In this framework, BCx contribution during early consolidation (my case) may well be redundant, because a vast array of other cortical areas may contribute to uphold the memory in parallel. Thus, in case of BCx blockade, these other contributors may be sufficient to maintain the learned response, explaining my result of BCx dispensability in this phase. Future studies need to test effects of BCx blockade later during late consolidation to test whether BCx is part of the set of cortical nodes responsible for final TTEBC memory.

In contrast to the critical role of BCx for TTEBC acquisition, delay conditioning of the same reflex is independent of BCx. Is it then that cortex is obligatorily required whenever short term memory functions are needed to accomplish the associations? Within simple EBC paradigms this may well be the case. However, a survey of known facts from other learning paradigms quickly reveals that this statement is not valid in its exclusive form: That is, the statement that cortex is needed whenever short term memory is required may well be true, but its reverse, that whenever cortex is required the reason is to provide short term memory function, is false. One example supporting this statement is delay eye blink conditioning. Clarke and Squire found that humans develop awareness about the task contingencies but the expression of conditioned responses do not require short term memory functions and follow simple laws of association strength (Clark *et al.*, 2001). In delay EBC, therefore, cortex contribution may go along with awareness of task contingencies (easily accessible in humans by asking them) – but not with association of CS and CR (measured by assessing e.g. the CR ratio). A second example showing that cortex contribution is not always driven by requirement of short-term memory, is delay fear conditioning (FC). FC is a classic parading of association learning, in which a neutral stimulus is paired with a strongly aversive stimulus (e.g. electric foot shocks, innate fear evoking smells, etc.). Despite the fact, that FC is commonly realized as a delay paradigm, and in contrast to delay EBC, it has been found to be dependent on different parts of cortex, ranging from hippocampus to PFC and even secondary sensory cortices (Sacco & Sacchetti, 2010; Maren *et al.*, 2013; Raybuck & Lattal, 2014). Contribution of cortex in FC has been attributed to various facets of the tasks, like complex contexts, or emotional content (Grosso *et al.*, 2015), and is commonly linked to awareness of fear, while the automatic, reflexive behavior is linked to the amygdala (LeDoux, 2014). Nevertheless, a parallel between FC and EBC paradigms seems to emerge from recent studies that compared delay and trace versions of FC. Trace FC recruits additional hippocampal and cortical areas in comparison to delay FC (Raybuck & Lattal, 2014). In conclusion, cortex generally seems to contribute a cognitive component to learning of delay and trace type conditioning. For complex paradigms (e.g. context sensitive delay FC) cortical recruitment may be triggered by several factors including short term memory requirement (Kim *et al.*, 2013). In simple tasks – like the present single context TTEBC paradigm – cortex attains critical importance for CS-US/CR associations only when short term memory is required.

Neuronal correlate of TTEBC

The present results demonstrate that TTEBC acquisition is accompanied by a temporally specific decrement (in late CS & trace period) of BCx spike and LFP activity. The time course of this specific learning-related suppression, which continues across the five learning sessions, parallels the known time course of plastic changes of spines observed on L5 apical dendrites (Joachimsthaler *et al.*, 2015). There is, however, the problem that the learning-related changes in spine numbers and neuronal activity continued up to the period of expression of learning (retention), in which, as mentioned, neither the acute (present study) nor previous chronic blockade (Galvez *et al.*, 2007; Galvez *et al.*, 2011) abolished the learned behavior. Can the assumption of a causal role of the morphological and activity changes be upheld in face of these results? I think the answer is yes. The observed mismatch between results from correlative and manipulative experimental strategies does not exclude the presumed causal role. As discussed above, there is reason to think that during early consolidation multiple cortical areas play a shared causal role which would prevent that blockade of one of the contributing structures alone can block the learned content. In this sense the learning-related changes in BCx could be part of a causally relevant but redundant system during that phase. Later during consolidation, as discussed above, the contribution of cortical areas may be pruned. This idea motivates future studies to find out firstly, whether BCx is amongst those areas that keep the consolidated memory, and thus may regain a critical role for retention late after learning, and secondly, to investigate other cortical areas possibly contributing to early consolidation.

Several studies that monitored primary sensory cortex activity during association learning support my finding that evoked responses are attenuated during learning. Miller et al., (2008) discovered that visual trace conditioning reduces CS responses in a primary visual sensory cortex, in rabbits. Gdalyahu et al. (2012) found, that fewer L2/3 mouse BCx neurons respond to the CS, 4–5 days after associative tactile fear learning. One earlier finding using TTEBC in rabbits, however, apparently diverged from the present results (Ward *et al.*, 2012). The difference in findings of this earlier study is, firstly, an enhancement in the *short* latency CS response (only in BCx L5/6 infragranular neurons, other layers were not studied) - the response period that was unchanged in the present study. Secondly, the Ward *et al*. study used a group of pseudo-conditioned animals for comparison while the present study used CSD and MU data to perform the more sensitive within-group comparisons. Additionally, the spike densities gained from pseudo-conditioned and conditioned groups in the Ward *et al*., study showed a clear and consistent decrease of baseline firing rate in the conditioned group. In comparisons of z scores between the two groups these changes may well have played a role to bring out reported differences between the two groups. Further, the number of significantly responding units was decreased in the conditioned group (while those that responded showed a greater change in firing rate), a fact that may have been underestimated in my CSD and MU recordings. Future experiments using pseudo-conditioned and single unit data throughout the layers will be needed to clarify these apparent deviating effects.

VGAT-ChR2-eYFP mouse line senses transient optogenetic BCx blockade

As a side note, I found indications, that the VGAT-ChR2-eYFP mouse line senses optogenetic perturbation. Surprisingly, the local activation of GABAergic interneurons in BCx was sufficient to work as a CS in about half of the animals. The VGAT-ChR2-eYFP mouse line is frequently used in experiments, but no one ever reported their ability to perceive cortical light perturbance. How mice sense the optogenetic perturbation is unclear, because inhibitory effects are largely limited to a cortical column, i.e. there is no long range inhibition in Cx. One possibility is that, against an otherwise tonic activity a depression in firing rate might be discriminated. Indeed, Kiritani *et al.* (2016), working in motor cortex, reported the interesting observation that BCx inactivation in VGAT mice causes suppression of whisking by rapid hyperpolarization and spike suppression in L2/3 and L5. The implications of my discovery, that Cx inactivation can be perceived, for previous and future studies in the VGAT (and other similar mouse lines) will require further evaluation. In this study I avoided entanglement in these problems as mice sensitive to optogenetic blockade did not enter the data set.

TTEBC generalization across whiskers

This is the first report about the generalization of TTEBC learned content to other untrained whiskers. I find that mice have generalized associations only to directly neighboring whiskers. This result fits nicely with that of other studies, suggesting that mice and rats generalize to adjacent, but not far whiskers in a fear conditioning (Gdalyahu *et al.*, 2012), and a gap-crossing (Harris *et al.*, 1999) paradigm. Notably, the extend of this generalization to the direct neighboring whiskers corresponds well with the extent of axonal arborization into adjacent columns of L5 thick tufted pyramidal neurons (Oberlaender *et al.*, 2011). The neurons known to loose L1 spines during TTEBC represent a subset of these cells (Joachimsthaler *et al.*, 2015). The match of generalization across whiskers with barrel column cellular morphology, firstly suggests that BCx may be the causal substrate for generalization to adjacent whiskers, and on the same token, strengthens the notion that BCx underpins TTEBC acquisition. In future experiments, TTEBC generalization could be used as an additional tool to test the dependency of TTEBC on BCx intactness. Additionally, delay EBC could be employed to study whether, there as well, BCx blockade discriminates between learning of the task and its generalization to non-trained whiskers. On a more detailed level, single cell inactivation (e.g. blockade of the apical tuft of L5 neurons as done in Takahashi *et al.*, 2016) could be tried to elucidate the role of L5 apical tufts in whisker generalization.

Cortex and cerebellum both store the CS-US association for different purposes.

My study shows for the first time that barrel cortex holds specific activity during the trace period. This activity is independent of sensory input, as the whisker by definition is not deflected by the actuator in the trace period and the mice do not obviously move their whiskers during this period. The polarity in the CSD analysis (sinks during CS and source during trace) and the different spatial outline (reversal of CS-sinks in layer 2, reversal of trace-source not visible) are strong additional arguments against the notion that trace activity is of tactile origin. Most likely then BCx trace activity is of central origin. In fact, it has been shown that mPFC holds spike activity during the trace period that is likely projected to the precerebellar pontine nuclei (Siegel *et al.*, 2011; Siegel & Mauk, 2013; Siegel, 2014). In the cerebellum the trace activity is thought to be associated with US signals and takes control over the CR

(Woodruff-Pak & Disterhoft, 2008). Thus, in the simplest case, trace activity in BCx is a direct reflection of that known to exist in PFC or cerebellum. This hypothesis has to be tested using future inactivation experiments in the mentioned structures together with recordings in BCx.

Importantly, my optogenetic blockade unequivocally shows that BCx trace activity is non-critical for task acquisition. A similar test is lacking so far for mPFC or cerebellum (which both block TEBC when lesioned as discussed below). It can be safely assumed however, that in those brain structures projecting trace signals to the cerebellum (where it is thought to be used for association), the trace signal must attain a critical role for learning. After all, without the trace signal, association of CS and US is untenable, at least assuming the known temporal constraints governing synaptic plasticity (spike time dependent synaptic plasticity) that is at the basis of learning (Abbott & Nelson, 2000). I therefore predict that optogenetic approaches to discriminate the role of CS vs. trace activity, applied to mPFC and/or cerebellum will reveal a critical role of the respective trace activity.

I can only speculate which function the found trace activity in BCx has. Trace activity is key to associate CS and US in the trace paradigm. If I accept the notion of Clark *et al*. (2001), as discussed above, that TTEBC can be dissected into two basic functions, (1) the sensorimotor behavior and (2) the creation of awareness about task contingencies, then it becomes important to understand where the trace activity is created that is required for both systems. Available evidence strongly suggests that trace activity is generated only in one of these two parallel systems, namely the cortex, particularly in the mPFC, which projects it down to the cerebellum via the cortico-pontine pathway (Siegel *et al.*, 2011). This is the key feature linking the two association systems and nicely explains why cortex function is indispensable for trace learning. The dispensability of BCx trace activity for TTEBC, which exclusively reads out the ‘sensorimotor’ function (the generation of CRs) NOT the awareness function, points to the possibility that BCx trace activity exclusively takes part in the awareness function. In contrast BCx persistent-CS period activity may be part of both functions as indicated by abolished TTEBC during its blockade. A likely scenario is that persistent CS activity helps to establish trace activity in mPFC early during acquisition. In this framework BCx trace activity may well have important functions, e.g. to inform the learning subject of tactile characteristics of CS as well as temporal properties of the CS-US contingency. This view predicts that future experiments in mice establishing a read out of the created awareness, - e.g. measuring the response to extinction trials as established by Clark et al. (2001) – might well reveal effects of BCx lesions.

Previous models of TEBC (e.g. Woodruff-Pak and Disterhoft, 2008) would have the US signals only project to the cerebellum. In the framework of the two association systems, the US is also needed on the cortical level. A further argument for an additional pathway feeding US signals to cortex is the fact that BCx synapses undergo functional (present study) as well as morphological plasticity in response to CS-US pairings (Galvez, 2006; Galvez *et al.*, 2011; Chau *et al.*, 2014; Joachimsthaler *et al.*, 2015). For spike time dependent plasticity, the standard model for Hebbian synaptic plasticity in neocortex, the signals that are to be associated must arrive within a window smaller than 50ms (Abbott and Nelson, 2000). The question therefore arises how US signals arrive in cortex in time to be associated with the CS. A first possibility is the ascending tactile pathway originating with primary afferents in the cornea. This possibility is viable but has not been explored so far. It is left to future experiments to clarify the role of the somatosensory cornea representations for TTEBC. A second possibility is that US signals from the cerebellum arrive at the BCx. As the cerebellar nuclei (the output structure of the cerebellar complex) do not directly project to tactile thalamic nuclei (Schwarz & Thier, 1999), the exact pathway for such an interaction remains to be elucidated. A final possible pathway has been already intensely investigated as a neuronal pathway underpinning FC and TTEBC: Acetylcholinergic (ACh) projections originating from the nucleus basalis (NB) terminate in vast cortical areas including primary sensory areas. This afferent system to cortex is triggered by attention and salient stimuli (Rasmusson, 2000; Sarter *et al.*, 2005; Angela & Dayan, 2005; Flores & Disterhoft, 2009). In fact, Flores & Disterhoft (2009) reported that TTEBC acquisition facilitates NB responses to CS, and bilateral NB lesions impair learning in rabbits. In FC, NB activity has been shown to enhance learning (using auditory CS) and reshape receptive field characteristics in auditory cortex via disinhibition of L1 (Froemke *et al.*, 2007; Letzkus *et al.*, 2011). Antagonizing ACh receptors in primary auditory cortex reduces auditory fear conditioning (Letzkus *et al.*, 2011). Moreover, learning-related plasticity exists in NB itself, occurring after only 5 CS-US pairings, and precedes auditory cortex modifications (Maho *et al.*, 1995). Lastly, association related, acetylcholinergic NB synapses terminate on primary sensory cortical neurons in L1 (Kristt, 1979; Buzsaki *et al.*, 1988; Letzkus *et al.*, 2011). It might therefore play a role for the substantial loss of spines during TTEBC found in this layer (Joachimsthaler *et al.*, 2015). Certainly, it is possible that all or several mentioned US pathways contribute to TTEBC function and are involved with potential different functional aspects. For instance, the pathway via the S1 cornea representation may trigger modality specific plasticity while the NB pathway may support a more basic function providing attentional elements needed to initiate activation of widespread cortical areas including the mPFC and hippocampal circuits.

In summary, the present results help to shape the view that TTEBC is a complex task that contains components that can be classified as declarative memory, the ‘awareness system’ housed in the cortex, as well as the automated, reflexive memory, rooted in the cerebellar ‘sensorimotor system’. The two systems are linked in hierarchical ways, in that the cerebellar one is dependent on the trace activity provided by cortex. The cerebellar circuits are well known from classic studies (e.g. Woodruff-Pak and Disterhoft, 2008). BCx contribution to TTEBC as shown here has begun to reveal and dissect parts functionally exclusive to the cortical association network.

Citations

ABBOTT, L.F. & NELSON, S.B. 2000. Synaptic plasticity: taming the beast. *Nat Neurosci*.

ANGELA, J.Y. & DAYAN, P. 2005. Uncertainty, neuromodulation, and attention. *Neuron*, **46**, 681–692.

BARBERINI, C.L., MORRISON, S.E., SAEZ, A., LAU, B. & SALZMAN, C.D. 2012. Complexity and Competition in Appetitive and Aversive Neural Circuits. *Frontiers in Neuroscience*, **6**, 170, 10.3389/fnins.2012.00170.

BOSMAN, L.W.J., HOUWELING, A.R., OWENS, C.B., TANKE, N., SHEVCHOUK, O.T., RAHMATI, N., TEUNISSEN, W.H.T., … DE ZEEUW, C.I. 2011. Anatomical Pathways Involved in Generating and Sensing Rhythmic Whisker Movements. *Frontiers in Integrative Neuroscience*, **5**, 53, 10.3389/fnint.2011.00053.

BUZSAKI, G.Y., BICKFORD, R.G., PONOMAREFF, G., THAL, L.J., MANDEL, R. & GAGE, F.H. 1988. Nucleus basalis and thalamic control of neocortical activity in the freely moving rat. *J Neurosci*, **8**, 4007–4026.

CHAKRABARTI, S. & ALLOWAY, K.D. 2006. Differential origin of projections from SI barrel cortex to the whisker representations in SII and MI. *The Journal of Comparative Neurology*, **498**, 624–636, 10.1002/cne.21052.

CHAU, L.S., PRAKAPENKA, A. V., ZENDELI, L., DAVIS, A.S. & GALVEZ, R. 2014. Training-dependent associative learning induced neocortical structural plasticity: A trace eyeblink conditioning analysis. *PLoS ONE*, **9**, 1–8, 10.1371/journal.pone.0095317.

CHRISTIAN, K.M. & THOMPSON, R.F. 2003. Neural Substrates of Eyeblink Conditioning: Acquisition and Retention. *Learning & Memory* , **10**, 427–455 Available at: http://learnmem.cshlp.org/content/10/6/427.abstract.

CLARK, R.E., MANNS, J.R. & SQUIRE, L.R. 2001. Trace and Delay Eyeblink Conditioning: Contrasting Phenomena of Declarative and Nondeclarative Memory. *Psychological Science*, **12**, 304–308, 10.1111/1467-9280.00356.

CLARK, R.E. & SQUIRE, L.R. 1998. Classical conditioning and brain systems: the role of awareness. *Science*, **280**, 77–81.

CONSTANTINOPLE, C.M. & BRUNO, R.M. 2013. Deep Cortical Layers Are Activated Directly by Thalamus. *Science*, **340**, 1591–1594, 10.1126/science.1236425.

DENARDO, L.A., BERNS, D.S., DELOACH, K. & LUO, L. 2015. Connectivity of mouse somatosensory and prefrontal cortex examined with trans-synaptic tracing. *Nat Neurosci*, **18**, 1687–1697 Available at: http://dx.doi.org/10.1038/nn.4131.

DÖRFL, J. 1985. The innervation of the mystacial region of the white mouse: A topographical study. *Journal of Anatomy*, **142**, 173.

EBARA, S., KUMAMOTO, K., MATSUURA, T., MAZURKIEWICZ, J.E. & RICE, F.L. 2002. Similarities and differences in the innervation of mystacial vibrissal follicle–sinus complexes in the rat and cat: A confocal microscopic study. *The Journal of Comparative Neurology*, **449**, 103–119, 10.1002/cne.10277.

FELDMEYER, D. 2012. Excitatory neuronal connectivity in the barrel cortex. *Frontiers in Neuroanatomy*, **6**, 24, 10.3389/fnana.2012.00024.

FLORES, L.C. & DISTERHOFT, J.F. 2009. Caudate Nucleus Is Critically Involved in Trace Eyeblink Conditioning. *Journal of Neuroscience*, **29**, 14511–14520, 10.1523/JNEUROSCI.3119-09.2009.

FRANKLAND, P.W. & BONTEMPI, B. 2005. The organization of recent and remote memories. *Nature reviews. Neuroscience*, **6**, 119–130, 10.1038/nrn1607.

FROEMKE, R.C., MERZENICH, M.M. & SCHREINER, C.E. 2007. A synaptic memory trace for cortical receptive field plasticity. *Nature*, **450**, 425–429, 10.1038/nature06289.

GAGLIANO, M., RENTON, M., DEPCZYNSKI, M. & MANCUSO, S. 2014. Experience teaches plants to learn faster and forget slower in environments where it matters. *Oecologia*, **175**, 63–72, 10.1007/s00442-013-2873-7.

GALVEZ, R. 2006. Vibrissa-Signaled Eyeblink Conditioning Induces Somatosensory Cortical Plasticity. *Journal of Neuroscience*, **26**, 6062–6068, 10.1523/JNEUROSCI.5582-05.2006.

GALVEZ, R., CUA, S. & DISTERHOFT, J.F. 2011. Age-related deficits in a forebrain-dependent task, trace-eyeblink conditioning. *Neurobiology of Aging*, **32**, 1915–1922, http://dx.doi.org/10.1016/j.neurobiolaging.2009.11.014.

GALVEZ, R., WEIBLE, A.P. & DISTERHOFT, J.F. 2007. Cortical barrel lesions impair whisker-CS trace eyeblink conditioning. *Learning & memory (Cold Spring Harbor, N.Y.)*, **14**, 94–100, 10.1101/lm.418407.

GAMZU, E. & AHISSAR, E. 2001. Importance of Temporal Cues for Tactile Spatial- Frequency Discrimination. *Journal of Neuroscience*, **21**, 7416–7427 Available at: http://www.jneurosci.org/content/21/18/7416.

GDALYAHU, A., TRING, E., POLACK, P.-O., GRUVER, R., GOLSHANI, P., FANSELOW, M.S., SILVA, A.J. & TRACHTENBERG, J.T. 2012. Associative Fear Learning Enhances Sparse Network Coding in Primary Sensory Cortex. *Neuron*, **75**, 121–132, http://dx.doi.org/10.1016/j.neuron.2012.04.035.

GIURFA, M. 2015. Learning and cognition in insects. *Wiley Interdisciplinary Reviews: Cognitive Science*, **6**, 383–395, 10.1002/wcs.1348.

GREEN, D.M. & SWETS, J.A. 1966. Signal detection theory and psychophysics. *Signal detection theory and psychophysics*. New York: Wiley.

GRINVALD, A., LIEKE, E., FROSTIG, R.D., GILBERT, C.D. & WIESEL, T.N. 1986. Functional architecture of cortex revealed by optical imaging of intrinsic signals. *Nature*, **324**, 361–364 Available at: http://dx.doi.org/10.1038/324361a0.

GROSSO, A., CAMBIAGHI, M., CONCINA, G., SACCO, T. & SACCHETTI, B. 2015. Auditory cortex involvement in emotional learning and memory. *Neuroscience*, **299**, 45–55, 10.1016/j.neuroscience.2015.04.068.

GUO, Z., LI, N., HUBER, D., OPHIR, E., GUTNISKY, D., TING, J., FENG, G. & SVOBODA, K. 2014a. Flow of cortical activity underlying a tactile decision in mice. *Neuron*, **81**, 179–194, 10.1016/j.neuron.2013.10.020.

GUO, Z. V, HIRES, S.A., LI, N., O'CONNOR, D.H., KOMIYAMA, T., OPHIR, E., HUBER, D., … SVOBODA, K. 2014b. Procedures for behavioral experiments in head-fixed mice. *PloS one*, **9**, e88678, 10.1371/journal.pone.0088678.

HARRIS, J. A, PETERSEN, R.S. & DIAMOND, M.E. 1999. Distribution of tactile learning and its neural basis. *Proceedings of the National Academy of Sciences of the United States of America*, **96**, 7587–7591, 10.1073/pnas.96.13.7587.

HELMSTETTER, F.J. & BELLGOWAN, P.S. 1994. Effects of muscimol applied to the basolateral amygdala on acquisition and expression of contextual fear conditioning in rats. *Behavioral neuroscience*, **108**, 1005–1009.

HENKE, K. 2010. A model for memory systems based on processing modes rather than consciousness. *Nat Rev Neurosci*, **11**, 523–532 Available at: http://dx.doi.org/10.1038/nrn2850.

HENTSCHKE, H., HAISS, F. & SCHWARZ, C. 2006. Central Signals Rapidly Switch Tactile Processing in Rat Barrel Cortex during Whisker Movements. *Cerebral Cortex*, **16**, 1142–1156 Available at: http://dx.doi.org/10.1093/cercor/bhj056.

JOACHIMSTHALER, B., BRUGGER, D., SKODRAS, A. & SCHWARZ, C. 2015. Spine Loss in Primary Somatosensory Cortex during Trace Eyeblink Conditioning. *Journal of Neuroscience*, **35**, 3772–3781, 10.1523/JNEUROSCI.2043-14.2015.

JONES, M.S. & BARTH, D.S. 1999. Spatiotemporal Organization of Fast (>200 Hz) Electrical Oscillations in Rat Vibrissa/Barrel Cortex. *Journal of Neurophysiology*, **82**, 1599–1609 Available at: http://jn.physiology.org/content/82/3/1599.

KAJIKAWA, Y. & SCHROEDER, C.E. 2011. How local is the local field potential? *Neuron*, **72**, 847–858, 10.1016/j.neuron.2011.09.029.

KIM, E.J., KIM, N., KIM, H.T. & CHOI, J.-S. 2013. The prelimbic cortex is critical for context-dependent fear expression. *Frontiers in behavioral neuroscience*, **7**, 73, 10.3389/fnbeh.2013.00073.

KIM, J.J. & FANSELOW, M.S. 1992. Modality-specific retrograde amnesia of fear. *Science (New York, N.Y.)*, **256**, 675–677.

KIRITANI, T., GALAN, K., SREENIVASAN, V., ESMAEILI, V., KIRITANI, T., GALAN, K., CROCHET, S. & PETERSEN, C.C.H. 2016. Movement Initiation Signals. *Neuron*, **92**, 1368–1382, 10.1016/j.neuron.2016.12.001.

KORALEK, K.-A., OLAVARRIA, J. & KELLACKEY, H.P. 1990. Areal and laminar organization of corticocortical projections in the rat somatosensory cortex. *The Journal of Comparative Neurology*, **299**, 133–150, 10.1002/cne.902990202.

KRISTT, D.A. 1979. Development of neocortical circuitry: Histochemical localization of acetylcholinesterase in relation to the cell layers of rat somatosensory cortex. *The Journal of Comparative Neurology*, **186**, 1–15, 10.1002/cne.901860102.

LANGER, D., VAN 'T HOFF, M., KELLER, A.J., NAGARAJA, C., PFÄFFLI, O.A., GÖLDI, M., KASPER, H. & HELMCHEN, F. 2013. HelioScan: A software framework for controlling in vivo microscopy setups with high hardware flexibility, functional diversity and extendibility. *Journal of Neuroscience Methods*, **215**, 38–52, http://dx.doi.org/10.1016/j.jneumeth.2013.02.006.

LEDOUX, J.E. 2014. Coming to terms with fear. *Proceedings of the National Academy of Sciences*, **111**, 2871–2878.

LESKI, S., LIND??N, H., TETZLAFF, T., PETTERSEN, K.H. & EINEVOLL, G.T. 2013. Frequency Dependence of Signal Power and Spatial Reach of the Local Field Potential. *PLoS Computational Biology*, **9**, 10.1371/journal.pcbi.1003137.

LETZKUS, J.J., WOLFF, S.B.E., MEYER, E.M.M., TOVOTE, P., COURTIN, J., HERRY, C. & LÜTHI, A. 2011. A disinhibitory microcircuit for associative fear learning in the auditory cortex. *Nature*, **480**, 331–335, 10.1038/nature10674.

LINDÉN, H., TETZLAFF, T., POTJANS, T.C., PETTERSEN, K.H., GRÜN, S., DIESMANN, M. & EINEVOLL, G.T. 2011. Modeling the Spatial Reach of the {LFP}. *Neuron*, **72**, 859–872, http://dx.doi.org/10.1016/j.neuron.2011.11.006.

LOVICK, T.A. & ZBROZYNA, A.W. 1975. Responses to corneal stimulation in the trigeminal nuclei. *The Journal of physiology*, **245**, 81P–82P.

MAHO, C., HARS, B., EDELINE, J.M. & HENNEVIN, E. 1995. Conditioned Changes in the Basal Forebrain - Relations With Learning-Induced Cortical Plasticity. *Psychobiology*, **23**, 10–25, 10.3758/BF03327054.

MAREN, S., PHAN, K.L. & LIBERZON, I. 2013. The contextual brain: implications for fear conditioning, extinction and psychopathology. *Nature Reviews Neuroscience*, **14**, 417–428.

MAUK, M.D. & THOMPSON, R.F. 1987. Retention of Classically-Conditioned Eyelid Responses Following Acute Decerebration. *Brain Research*, **403**, 89–95.

MCCORMICK, D. A., LAVOND, D.G., CLARK, G. A., KETTNER, R.E., RISING, C.E. & THOMPSON, R.F. 1981. The engram found? Role of the cerebellum in classical conditioning of nictitating membrane and eyelid responses. *Bulletin of the Psychonomic Society*, **18**, 103–105, 10.3758/BF03333573.

MEYER, H.S., EGGER, R., GUEST, J.M., FOERSTER, R., REISSL, S. & OBERLAENDER, M. 2013. Cellular organization of cortical barrel columns is whisker-specific. *Proceedings of the National Academy of Sciences of the United States of America*, **110**, 19113–19118, 10.1073/pnas.1312691110.

MILLER, M.J., WEISS, C., SONG, X., IORDANESCU, G., DISTERHOFT, J.F. & WYRWICZ, A.M. 2008. Functional magnetic resonance imaging of delay and trace eyeblink conditioning in the primary visual cortex of the rabbit. *The Journal of neuroscience : the official journal of the Society for Neuroscience*, **28**, 4974–4981, 10.1523/JNEUROSCI.5622-07.2008.

MILLER, M.W. & VOGT, B. A. 1984. Direct connections of rat visual cortex with sensory, motor, and association cortices. *The Journal of Comparative Neurology*, **226**, 184–202, 10.1002/cne.902260204.

MITZDORF, U. 1985. Current source-density method and application in cat cerebral cortex: investigation of evoked potentials and EEG phenomena. *Physiological reviews*, **65**, 37–100.

NARAYANAN, R.T., EGGER, R., JOHNSON, A.S., MANSVELDER, H.D., SAKMANN, B., DE KOCK, C.P.J. & OBERLAENDER, M. 2015. Beyond Columnar Organization: Cell Type- and Target Layer-Specific Principles of Horizontal Axon Projection Patterns in Rat Vibrissal Cortex. *Cerebral Cortex*, **25**, 4450–4468 Available at: http://dx.doi.org/10.1093/cercor/bhv053.

NASSER, H.M. & MCNALLY, G.P. 2013. Neural correlates of appetitive–aversive interactions in Pavlovian fear conditioning. *Learning & Memory* , **20**, 220–228 Available at: http://learnmem.cshlp.org/content/20/4/220.abstract.

NICHOLSON, C. & FREEMAN, J.A. 1975. Theory of current source-density analysis and determination of conductivity tensor for anuran cerebellum. *Journal of neurophysiology*, **38**, 356–368.

NORMAN, R.J., BUCHWALD, J.S. & VILLABLANCA, J.R. 1977. Classical conditioning with auditory discrimination of the eye blink in decerebrate cats. *Science*, **196**, 551–553 Available at: http://www.ncbi.nlm.nih.gov/pubmed/850800.

OBERLAENDER, M., BOUDEWIJNS, Z.S.R.M., KLEELE, T., MANSVELDER, H.D., SAKMANN, B. & DE KOCK, C.P.J. 2011. Three-dimensional axon morphologies of individual layer 5 neurons indicate cell type-specific intracortical pathways for whisker motion and touch. *Proceedings of the National Academy of Sciences*, **108**, 4188–4193, 10.1073/pnas.1100647108.

POTWOROWSKI, J., JAKUCZUN, W., ŁĘSKI, S. & WÓJCIK, D. 2012. Kernel Current Source Density Method. *Neural Computation*, **24**, 541–575, 10.1162/NECO_a_00236.

QUIROGA, R.Q., NADASDY, Z. & BEN-SHAUL, Y. 2004. Unsupervised spike detection and sorting with wavelets and superparamagnetic clustering. *Neural computation*, **16**, 1661–1687, 10.1162/089976604774201631.

RASMUSSON, D.D. 2000. The role of acetylcholine in cortical synaptic plasticity. *Behavioural brain research*, **115**, 205–218.

RAYBUCK, J.D. & LATTAL, K.M. 2014. Bridging the interval: theory and neurobiology of trace conditioning. *Behavioural processes*, **101**, 103–111.

SACCO, T. & SACCHETTI, B. 2010. Role of Secondary Sensory Cortices in Emotional Memory Storage and Retrieval in Rats. *Science*, **329**, 649–656, 10.1126/science.1183165.

SARTER, M., HASSELMO, M.E., BRUNO, J.P. & GIVENS, B. 2005. Unraveling the attentional functions of cortical cholinergic inputs: interactions between signal-driven and cognitive modulation of signal detection. *Brain Research Reviews*, **48**, 98–111.

SCHENDAN, H.E., SEARL, M.M., MELROSE, R.J. & STERN, C.E. 2003. An fMRI Study of the Role of the Medial Temporal Lobe in Implicit and Explicit Sequence Learning. *Neuron*, **37**, 1013–1025, http://dx.doi.org/10.1016/S0896-6273(03)00123-5.

SCHWARZ, C., HENTSCHKE, H., BUTOVAS, S., HAISS, F., STÜTTGEN, M.C., GERDJIKOV, T. V, BERGNER, C.G. & WAIBLINGER, C. 2010. The head-fixed behaving rat--procedures and pitfalls. *Somatosensory & motor research*, **27**, 131–148, 10.3109/08990220.2010.513111.

SCHWARZ, C. & THIER, P. 1999. Binding of signals relevant for action: towards a hypothesis of the functional role of the pontine nuclei. *Trends in Neurosciences*, **22**, 443–451, http://dx.doi.org/10.1016/S0166-2236(99)01446-0.

SIEGEL, J.J. 2014. Modification of persistent responses in medial prefrontal cortex during learning in trace eyeblink conditioning. *J Neurophysiol*, **112**, 2123–2137, 10.1152/jn.00372.2014.

SIEGEL, J.J., KALMBACH, B., CHITWOOD, R.A. & MAUK, M.D. 2011. Persistent activity in a cortical-to-subcortical circuit: bridging the temporal gap in trace eyelid conditioning. *Journal of Neurophysiology*, **107**, 50–64, 10.1152/jn.00689.2011.

SIEGEL, J.J. & MAUK, M.D. 2013. Persistent activity in prefrontal cortex during trace eyelid conditioning: dissociating responses that reflect cerebellar output from those that do not. *Journal of Neuroscience*, **33**, 15272–15284.

SIEGEL, J.J., TAYLOR, W., GRAY, R., KALMBACH, B., ZEMELMAN, B. V., DESAI, N.S., JOHNSTON, D. & CHITWOOD, R.A. 2015. Trace Eyeblink Conditioning in Mice Is Dependent upon the Dorsal Medial Prefrontal Cortex, Cerebellum, and Amygdala: Behavioral Characterization and Functional Circuitry. *eNeuro*, **2**, ENEURO.0051-14.2015, 10.1523/ENEURO.0051-14.2015.

SIMONS, D.J. 1978. Response properties of vibrissa units in rat SI somatosensory neocortex. *Journal of Neurophysiology*, **41**, 798–820 Available at: http://jn.physiology.org/content/41/3/798.

SIMONS, D.J. & WOOLSEY, T.A. 1979. Brain Research, 165 (1979) 327-332 ©. **165**, 327–332.

SWADLOW, H.A., GUSEV, A.G. & BEZDUDNAYA, T. 2002. Activation of a cortical column by a thalamocortical impulse. *The Journal of neuroscience : the official journal of the Society for Neuroscience*, **22**, 7766–7773.

TAKAHASHI, N., OERTNER, T.G., HEGEMANN, P. & LARKUM, M.E. 2016. Modulate Perception. **354**, 1159–1165, 10.1126/science.aah6066.

THOMPSON, R.F. 1990. Neural mechanisms of classical conditioning in mammals. *Philosophical transactions of the Royal Society of London. Series B, Biological sciences*, **329**, 161–170, 10.1098/rstb.1990.0161.

THOMSON, A.M. & BANNISTER, A.P. 2003. Interlaminar connections in the neocortex. *Cerebral cortex (New York, N.Y. : 1991)*, **13**, 5–14, 10.1093/cercor/13.1.5.

TSENG, W., GUAN, R., DISTERHOFT, J.F. & WEISS, C. 2004. Trace eyeblink conditioning is hippocampally dependent in mice. *Hippocampus*, **14**, 58–65, 10.1002/hipo.10157.

WARD, R.L., FLORES, L.C. & DISTERHOFT, J.F. 2012. Infragranular barrel cortex activity is enhanced with learning. *Journal of neurophysiology*, **108**, 1278–1287, 10.1152/jn.00305.2012.

WEISS, C. & DISTERHOFT, J.F. 2009. Use with Freely Moving Animals. *Journal of Neuroscience*, **173**, 108–113, 10.1016/j.jneumeth.2008.05.027.Evoking.

WOODRUFF-PAK, D.S. & DISTERHOFT, J.F. 2008. Where is the trace in trace conditioning? *Trends in neurosciences*, **31**, 105–112, 10.1016/j.tins.2007.11.006.

ZHAO, S., TING, J.T., ATALLAH, H.E., QIU, L., TAN, J., GLOSS, B., AUGUSTINE, G.J., … FENG, G. 2011. Cell type–specific channelrhodopsin-2 transgenic mice for optogenetic dissection of neural circuitry function. *Nature Methods*, **8**, 745–752, 10.1038/nmeth.1668.

ZOLA-MORGAN, S.M. & SQUIRE, L.R. 1990. The primate hippocampal formation: evidence for a time-limited role in memory storage. *Science*, **250**, 288–290.

Appendix

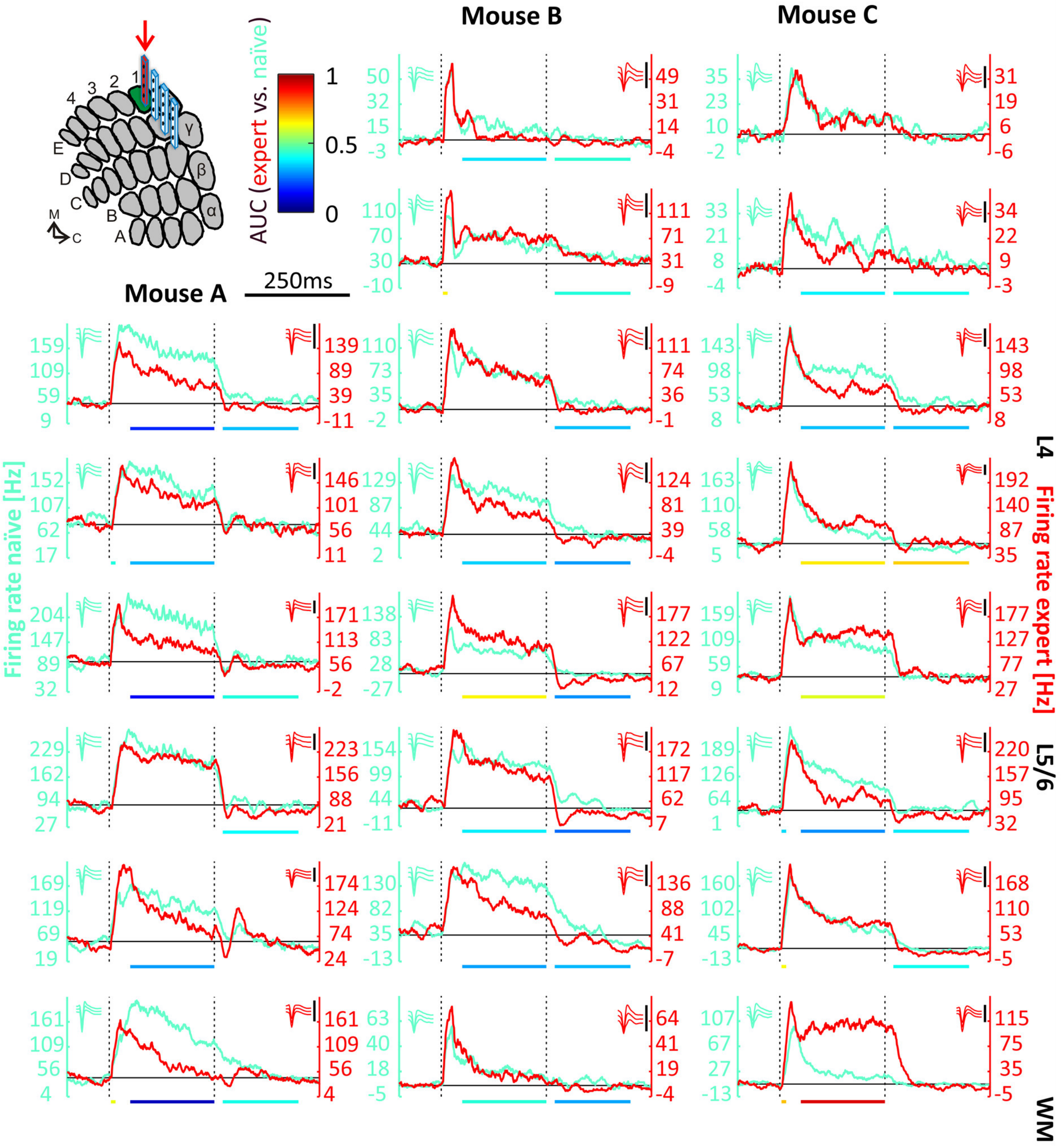

***Figure A1. MU activity on the first shank.**, i.e. located in the barrel column receiving the trained whisker (E1) (electrode shank marked by red arrow and highlighted in red). Naïve (turquoise; left ordinate) and expert (red; right ordinate) PSTHs across the principle barrel column of mouse A, B and C. Broken lines: CS on- and offset. Colored bars below abscissae indicate color-coded effect sizes (AUC, see color map next to barrel map) for CS onset, CS persistent and trace activity (cf. Fig. 12). Cortical layers L4 & L5/6 indicate relative cortical depths. Small insets: MU wave forms (±sd; scale bars: 50µV).*

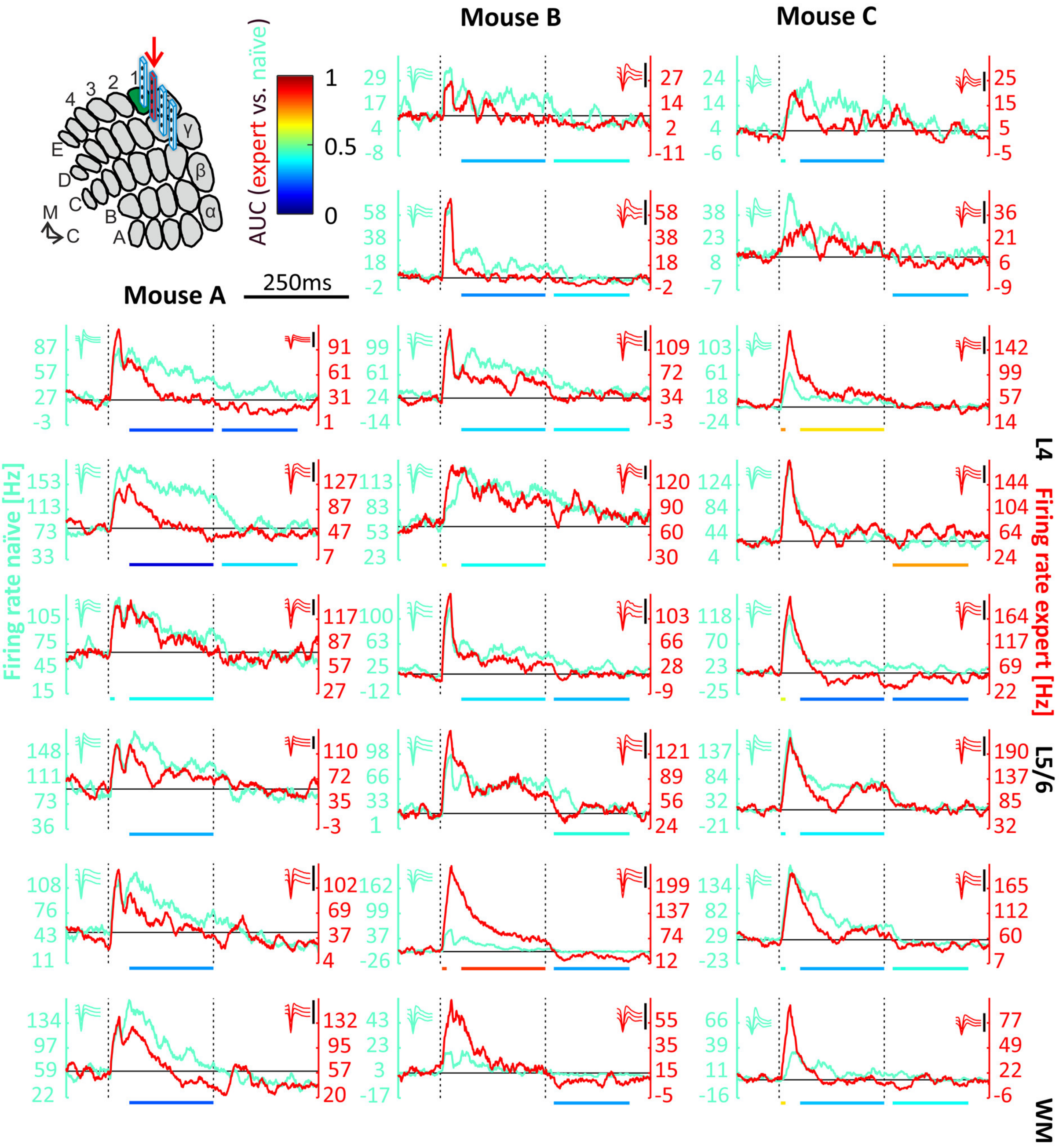

Figure A2. MU activity at a distance of 200µm *Conventions as in Figure A1.*

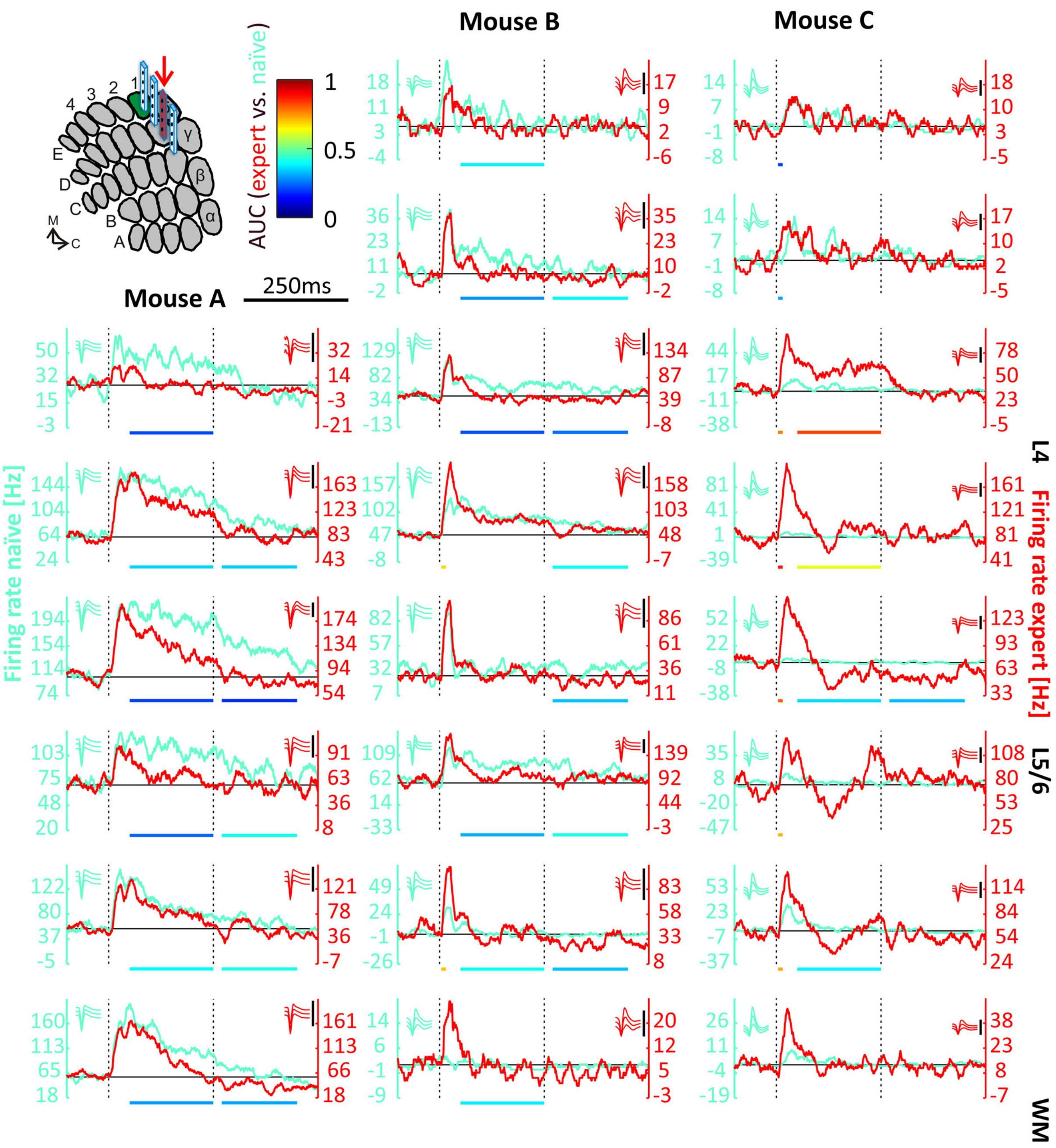

Figure A3. MU activity at a distance of 400µm *Conventions as in Figure A1.*

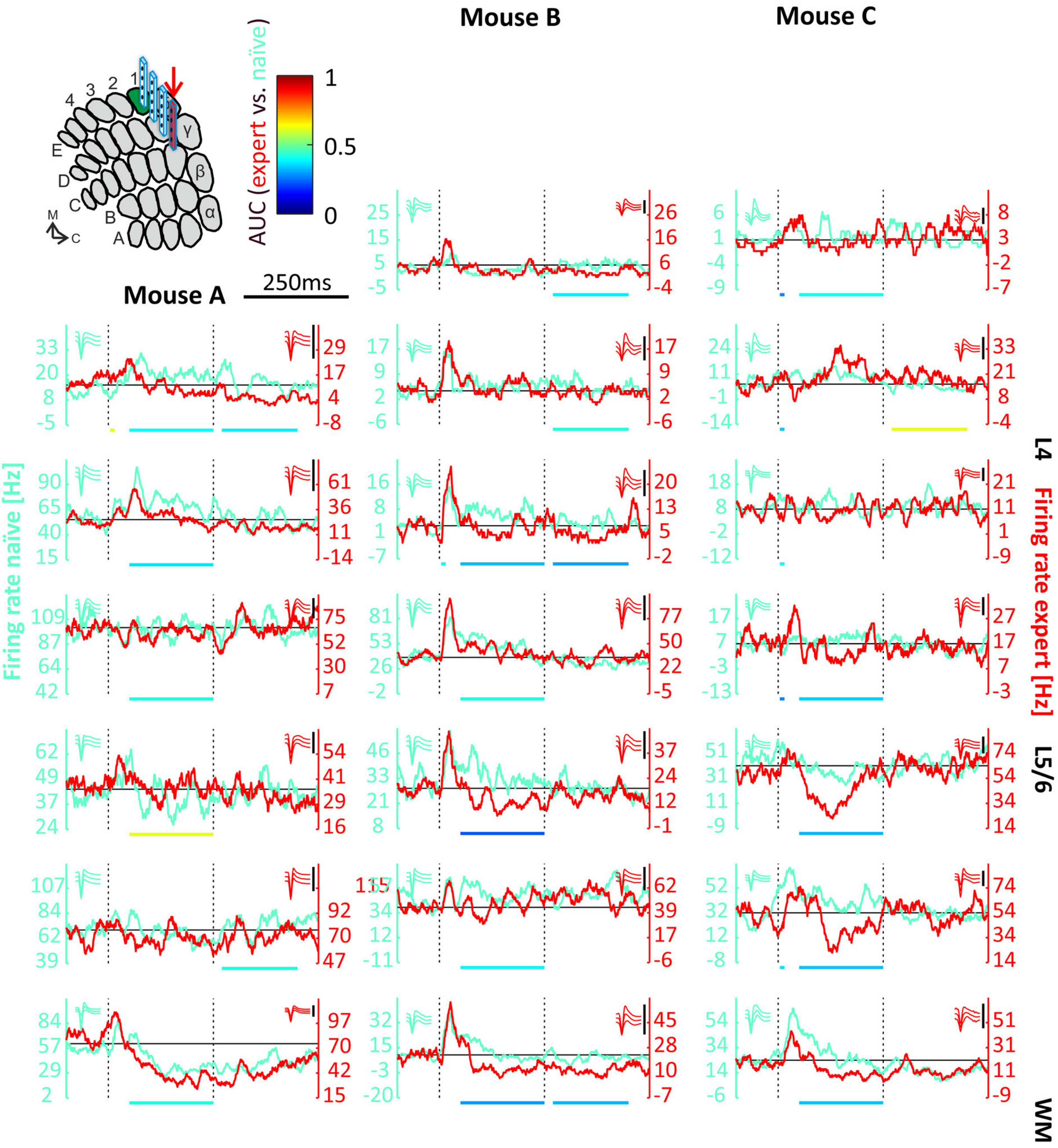

Figure A4. MU activity at a distance of 600µm *Conventions as in Figure A1.*